Comm.
Dr. Jacobson
Dr. Loosli
Dr. Sommers

CHRONIC PULMONARY DISEASE

No. 897
646-Act. 4/1/68
Ren. 4/1/69
4/1/70
646A-Act. 4/1/71
Ren. 4/1/72

THE COUNCIL FOR TOBACCO RESEARCH - U.S.A., INC.
110 EAST 59TH STREET
NEW YORK, N. Y. 10022

JAN 26 1973

Application For Research Grant

Date: October 13, 1973

1. Name of Investigator(s): (include Title and Degrees) Robert C. Rosan, M.D.
Associate Professor of Pathology and Pediatrics, St. Louis University
Associate Pathologist, Cardinal Glennon Memorial Hospital for Children,

2. Institution & Address: Cardinal Glennon Memorial Hospital for Children
1465 South Grand Boulevard
St. Louis, Missouri 63104

Checks to: Veljko Jellech
Chief Fund
Accountant

3. Short Title of Project:

Molecular parameters of lobular regeneration and function

4. Proposed Starting Date: April 1, 1973

5. Anticipated Duration of this Specific Study: Three years

6. Brief Descripton of Objectives or Specific Aims: In order to learn how chronic cellular injury in bronchioles leads to abnormal centrilobular repair, a novel quantitative model of irreversible lung injury will be evaluated through the correlation of molecular dissection with lung physiology, clinical and anatomical pathology, and roentgenography. Smoke is delivered by a Walton smoking machine.

1. The long-range goal: to develop predictive models of lung function after a specific irreversible injury to the small bronchioles.
2. The intermediate goal: to describe cellular alterations in the lung lobule that, after irreversible injury, lead to functional changes in ventilation.
3. The immediate goal: to describe selected processes of regeneration in the bronchiolar portion of the lung lobule after irreversible injury.

The selected processes include the cytoplasmic syntheses of these proteins, thought to typify the following events: glutamyl transpeptidase (cellular injury);[1] aspartic transcarbamylase (nuclear regeneration);[2] constitutive ribosomal protein (cytoplasmic regeneration);[3] alkaline phosphatase isoenzyme (differentiated mucosal activity).[4] These moities will be estimated in lung homogenates, histochemical stains, and peripheral blood. Lung function will be estimated primarily by a novel evaluation of pulmonary mixing.[5] Clearance function will be estimated with the same tantalum powder used for roentgenographic study.[6] After complete autopsies, lungs will be histologically evaluated by ordinal score technic[7] and goblet cell counts.[8] A special feature of the design is the attempted isolation of bronchiolar neurosecretory granules[9] by molecular dissection, and the correlation of results with lobular growth, function, and repair as measured above.

7. Give a Brief Statement of your Working Hypothesis: Irreversible lobular injury is associated with measurable changes in cellular and molecular differentiation of the lobule. (Technological advances, including automated enzyme analysis, zonal ultracentrifugation, advanced gas analysis systems, and multichannel physiological recording do permit a large-scale approach by an interdisciplinary team.)

1003538629

Source: https://www.industrydocuments.ucsf.edu/docs/hqyl0000

5

8. Details of Experimental Design and Procedures: (Attach Separate Pages)

This is a multidisciplinary design, in which the experimental animal inhales test material (oxygen or cigarette smoke), is followed by lung function studies (nitrogen washout and minute ventilation) and also by serum enzyme study (alkaline phosphatase isoenzymes, glutamyl transpeptidase, aspartic transcarbamylase) and hemograms; blood gases are measured in conjunction with the lung function studies. At autopsy, the lung tissue is itself studied for the molecular markers above, and as well for morphological variation which includes goblet cell counts and graded histology.

The essence of the design is that the animal is followed in the manner of a human patient. Multiple clinical, anatomical, radiological and biochemical variables are measured, and correlated with the progress of the lung disease.

9. Physical Facilities Available (Where Other than Administering Organization Indicate Geographical Location)

All physical facilities required are within Cardinal Glennon Memorial Hospital for Children, except for the electron microscopy which is carried out by collaboration with a commercial consultation service (Sperry Rand).

10. Additional Requirements:

The need for one item on the budget, the cryostat microtome IEC #398 @ $3,050 might be questioned at first glance; however, no such instrument is in our laboratory. Moreover, the surgical-autopsy facilities of Cardinal Glennon Hospital will be serving for a nearby 450 bed hospital while that hospital undergoes extensive remodeling. Under the circumstances, it would not be practical to add a research burden to the service load.

11. Biographical sketches of all principal and professional personnel (append)

12. List of publications: (Five most recent as pertinent) (append)

Asterisked in reference list.

10035388630

Source: https://www.industrydocuments.ucsf.edu/docs/hdyf0000

13. Budget: (1st year)

A. Salaries (Personnel by names)		% time	Amount
Professional			
	Robert C. Rosan, M.D.	10%	0.
Technical	George Pounds, BS (Clinical biologist)	100%	9,200.
	----------, BS (Physiologist)	100%	8,400.
	----------, BS (Chemist)	100%	8,400.
	Antoinette Cova, (Secretary)	25%	1,800.
	----------, BS (X-ray technician)	10%	840.
	Total Fringe on above		2,680.
		SUB-TOTAL	31,320.
B. Consumable Supplies (list by categories)			
	Guinea pig care and maintenance, 10¢/d x 40 pigs x 365 d		1,460.
	Miscellaneous Glassware		500.
	Miscellaneous Chemicals		750.
	Radionuclear supplies (for aspartyl transcarbamylase)		800.
		Sub-Total	3,510.
C. Other Expenses (itemize)			
	Pro-rated permanent equipment maintenance, 50%		750.
	Electron microscope consultant (Sperry Rand, 20 pictures x $55.00		1,100.
	Computer time (Hewlett-Packard 9800) $3.20/hr x 80 hr		256.
	Travel (To electron microscope consultant, Washington, DC x 2) . . .		369.
		Sub-Total	2,475.
D. Permanent Equipment (itemize)			
	Fluorescence-phase equipment to convert existent research microscope, Wilde M-20, Wilde Cat. #259-022, 243-395, 268-054, 268-022, 250-390, and 105-844		6,090.
	Fluorescence equipment to convert existent Coleman 129 spectrophotometer to fluorescence, Coleman Cat. #139-0251, 139-0481		1,775.
	Cryostat microtome, Damon Co. IEC #398		3,050.
	Ultracentrifuge rotor, Damon Co. IEC #494		800.
		SUB-TOTAL	11,715.
		TOTAL	49,020.
E. Overhead (15% of A+B+C)			
	E. Overhead (15% of A + B + C)	Total $5,595.00	
		TOTAL	54,615.

Estimated Future Requirements:

	Salaries	Consumable Suppl.	Other Expenses	Permanent Equip.	Overhead	Total
Year 2*	32,760	3,685	2,599	0	4,099	43,143
Year 3*	34,398	3,869	2,728	0	4,304	45,299

*Includes 5% annual cost-of living increases.

It is understood that the applicant and institutional officers in applying for a grant have read and found acceptable the Council's "Statement of Policy Containing Conditions and Terms Under Which Project Grants Are Made."

Signature [signature] M.D.
Director of Project Robert C. Rosan, M.D.
Telephone

Signature Sister Mary Helen Lyonnet Becker
Business Officer of the Institution
Telephone

10035386 31

Source: https://www.industrydocuments.ucsf.edu/docs/hgyl0000

Other Sources of Financial Support

List financial support for research from all sources, including own institution, for this and/or related research projects.

Current

	Title of Project	Source	Amount	Duration
NHLI RFP 72-25	Chronic pulmonary disease and smoking (animal model)	National Heart and Lung Institute (Contract)	$78,000.00	one year

ending: None

100353863

Source: https://www.industrydocuments.ucsf.edu/docs/hqyl0000

8. Details of Experimental Design and Procedures:

A. INTRODUCTION

For the past three years, The Council for Tobacco Research - U.S.A. (CTR) has supported our study of molecular and cellular alterations associated with growth, differentiation, and regeneration of injured human and animal lung. The results and significance of this work will be summarized below. As a direct recognition of these studies, we recently received a renewable competitive National Heart and Lung Institute (NIH) contract (RF #72-25) for $78,000 which establishes both the core team and the basic equipment to conduct a wide spectrum of experimental studies on irreversible bronchiolar injury. In this CTR proposal, we plan to use the new NIH experience in leap-frog fashion, that is, to apply the fully matured interdisciplinary approach which NIH now nourishes to the next phase of our CTR research. Furthermore, we expect that a "multiplier effect" may stimulate serendipitious advances when NIH and CTR groups are at work in experimental areas which are physically, intellectually, scientifically, and clinically contiguous portions of a dynamic biomedical landscape.

B. THE UNIT LOBULE HYPOTHESIS

The most important issue from previous CTR husbandry of our work is a new theory of lung growth, function, and repair, which I term the unit lobule hypothesis (Fig. 1).

In brief, the theory states that the lung functions as an assemblage of coordinated units, called unit lobules,[10] rather than as a mass organ. These lobules contain, in their apical regions, the regulatory mechanisms for lobular gas flow, perfusion of the microcirculation, and significantly, modulation of the milieu interieur of the parenchymal lung tissue.[10,11]

10035633

Source: http://www.industrydocuments.ucsf.edu/docs/[illegible]

FIGURE 1 FETAL/PREMATURE/NEONATAL UNIT LOBULE

BU Budding of bronchiole into primitive air sac

SE Secretory mucosa associated with tubular secretion/resorption

CL Clara cell

CI Ciliated cell

NE Nerve

KU Kultschitsky (neurosecretory) cell

AR Muscular arteriole

IN Intersaccular septum of bulky mesenchyme

DE Deep microcirculation of potential intrapulmonary shunts

AI Air-blood barrier

II Type II cell

MU Bronchiolar smooth muscle

LY Lymphatic in typical parabronchiolar position

WA Alveolar wall (juxtaposition of alveole and bronchiole)

RE Regulatory area of lobule containing active tissue

10035386634

Source: http://www.industrydocuments.ucsf.edu/tobacco

FIG. 1

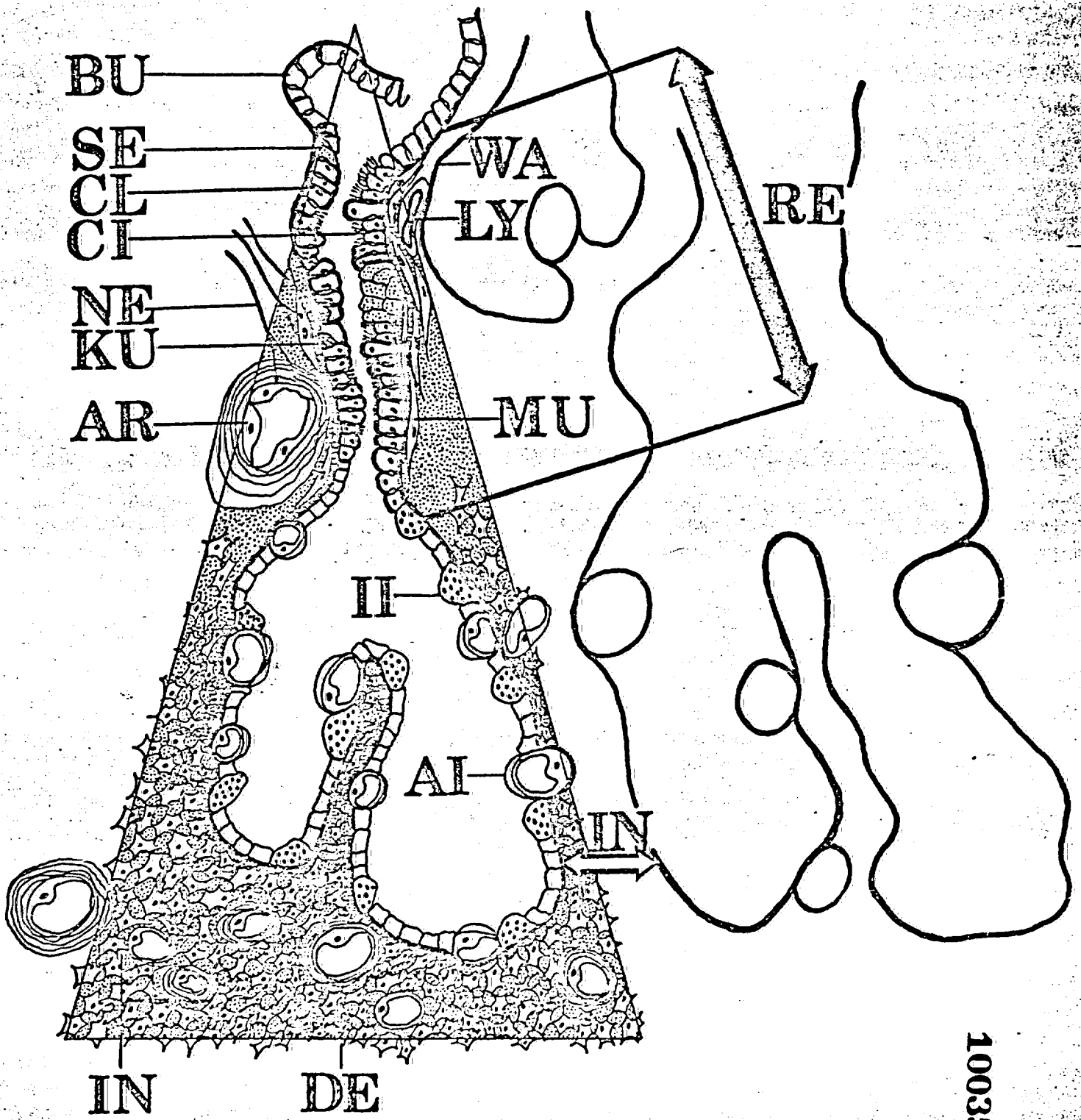

10035386 35

Source: https://www.industrydocuments.ucsf.edu/docs/hgyl0000

Fig. 2

The critical "regulatory region" of Fig. 1, as seen in a 600 g liveborn infant. Note the excellent development of arterioles, and the close association of bronchiolar smooth muscle with mucosa above and arteriole below. The loose, mesenchymal character of the peribronchiolar tissue is well seen. We believe this morphology helps explain the great compliance (see Fig. 28) and great susceptibility of neonatal bronchioles with respect to peribronchiolar edema.

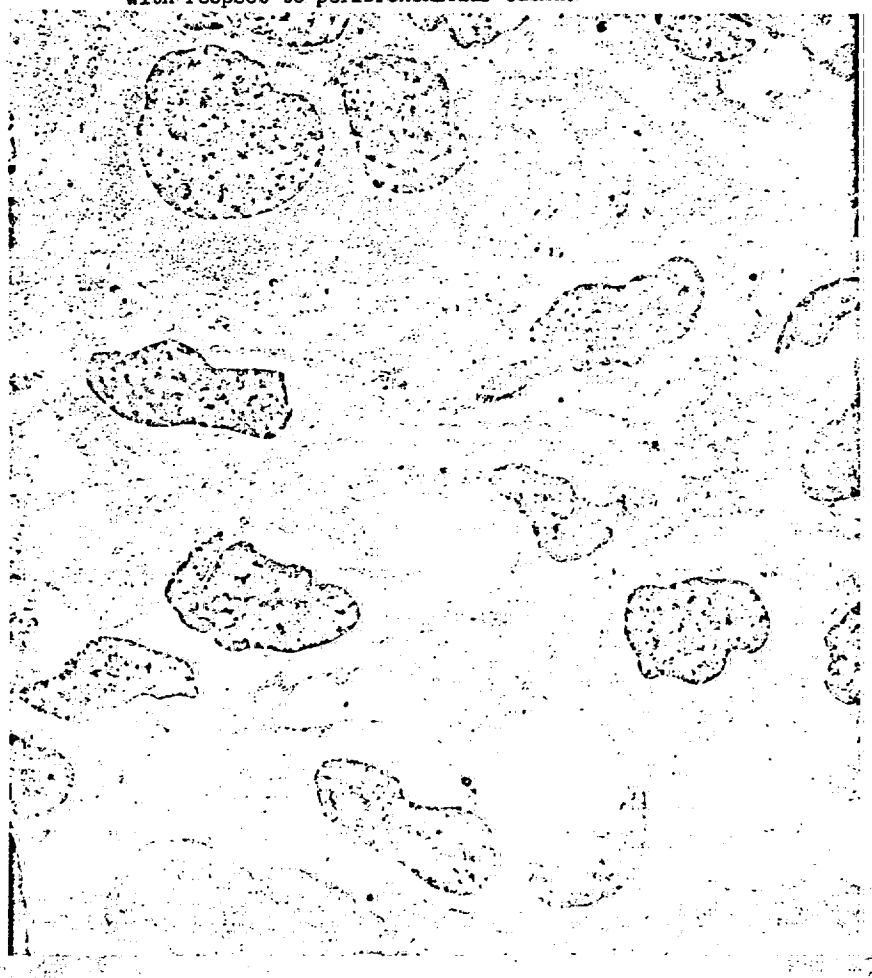

10035636

Source: https://www.industrydocuments.ucsf.edu/docs/hgyl0000

FIG. 3

The Unit Lobule Hypothesis

POSTULATION:

The basic functional module of the lung is the unit lobule, which consists of an apical regulatory region and a basal passive region.

COROLLARIES:

1. Bronchiolar compliance is a significant mechanical feature of apical lobular function which is subjected to continuous active regulation.
2. Homeostasis of the interstitium, including that of the basal passive region, is modulated by the apical regulatory region.
3. Effective function of the lobule is vested in the active process whereby the component functions are integrated.
4. Mass lung action is the product of integrated lobular function.
5. Regeneration of the injured lobule in part recapitulates its development.

10035386 37

Thus, the unit lobule consists of: (a) an apical regulatory region associated with neurogenic, muscular, endothelial, mucosal and lymphoid differentiation, and (b) a basal passive region, the vascular tissue lattice of the intra-alveolar septae (or in immature lungs, the intersaccular septae)[12] associated with a distinctive organoid, the air-blood barrier, a surfactant system and a macrophage system. That this hypothesis has been received with interest in the academic community may be judged by the evidence that we have been asked to contribute chapters to three books for three different audiences within one year,[13,14,15] and have had numerous requests for Fig. 1.

The first five corollaries implied by the unit lobule hypothesis follow. An obligative corollary and one of the particular novelties of this hypothesis is this: the bronchioles are among the most compliant portions of the lobule. This notion is in sharp relief to the established surfactant dogma of Clements, Avery, and others[16] but it is supported by the authoritative voices of Auerbach[17] and Thurlbeck,[18] by data of post-mortem babies from Strang's group,[19] by experimental and clinical studies of oxygen toxicity by ourselves[20,21] and others,[22] and by direct observations of Towers.[23] For the present, the chorus of these observations seems to constitute a rising crescendo. Our most recent observations on positive end-expiratory ventilation of babies, strongly supports these arguments (Fig. 28)[24] It is the active regulation of bronchiolar compliance which helps regulate lobular gas flow.

In a second corollary, we now propose that active airway control achieved by neuromuscular and mucosal mechanisms pari passu helps regulate the milieu interieur of parenchymal lung tissue through its effects on lymph flow in parabronchiolar lymph channels. Indeed, we believe that parenchymal homeostasis and airway mechanics are intimately interlocked. The advantage of

10035638

Source: https://www.industrydocuments.ucsf.edu/docs/fmgj0000

the well-known close association of peri-arteriolar and peri-bronchiolar smooth muscle with lymphatic channels is clear; but we believe that the bronchiolar mucosa itself actively participates in the exchange of fluids between the lumens of airways and the lobular interstitium. It was Clara who originally proposed the analogy of bronchiolar mucosae to renal tubular epithelia,[25] and none of the morphologic evidence of recent ultrastructural advances can contradict his idea.[11] Rather, the morphological adaptation of Clara cells (Fig. 3) suggests to us a specialization for (a) regulation of intercellular fluid exchange (b) intracellular synthesis of surface coat components (c) elaboration and translocation of other materials, e.g. those which subserve clearance and compliance, as well as other functions.[11]

A third corollary states that the function of the lobule is vested in the integration of its components. This contrasts again to the monolithic outlook of surfactant dogma. More importantly, and from the perspective of experimental design, from this corollary flows the claim that no single lobular parameter can be manipulated experimentally without inducing change in other of the functional components of the lobule. In effect, this corollary is the converse of a commonsense pathologists' observation: a wide variety of pulmonary insults produces a stereotyped monotony of responses. To paraphrase, a small number of final common pathways is implicit in the functional and molecular anatomy of the unit lobule. Thus, the lobule is a system, to be analyzed by systems analysis, and thus susceptible of computer modeling. However, a steady-state system must maintain its own equilibrium through feed-back control; hence, this corollary predicts that important lobular feedback controls exist.

1003538639

Source: https://www.industrydocuments.ucsf.edu/docs/fqgd0000

A fourth corollary states that, because the unit lobule is the fundamental module of functional lung anatomy, mass lung action is secured through the coordination of these units. Thus, the whole lung is also a system, and not the sum of its atomistic parts. Rather, the system is an expression of the activities of numerous unit lobules which are not necessarily completely synchronized nor completely equivalent. To demonstrate that this is indeed the mode by which the normal lung functions, one should be able to explain the well-known physiological data of normally encountered ventilation:perfusion inequities. We interpret certain observations of Lauweryns,[26] Towers,[23,27] Shanklin,[22] and others, and our own data on oxygen toxicity[20,21,28] that indeed it is normal for some lobules to be at work or in one phase of ventilation, while others are at rest or in a different phase.

The fifth and shortest corollary states that regeneration of the injured unit lobule in part recapitulates its normal ontogeny. It is this corollary for which the least data exist, and it is to this area of ignorance that our proposed activity is heavily directed.

For the purpose of this proposal, the main hypothesis and the five corollaries are tabulated in abbreviated form (Fig. 3). We anticipate that further experience may suggest modifications or even rejection of some of the above ideas, and count that as a beneficial result of an organized theoretical framework. On the other hand, we also anticipate that additional corollaries will suggest their presence when the experimental data are generated.

1003538640

Source: https://www.industrydocuments.ucsf.edu/docs/...

C. EXPERIMENTAL DESIGN

(1) Summary:

Guinea pigs under close clinical observation are challenged with controlled doses of oxygen or cigarette smoke delivered by a Walton smoking machine. Periodically, nitrogen wash-out is analyzed as a function of pulmonary mixing, minute ventilation is also evaluated, the peripheral blood is analyzed by means of a hemogram, the blood gases and pH are analyzed, and three test enzymes are estimated (see below). Prior to sacrifice, a bronchogram is arranged by tantalum particle technic and bronchiolar clearance is estimated by a follow-up radiograph. At autopsy, the lung is analyzed under three headings: lung homogenates are examined after sucrose gradient zonal ultracentrifugation for their ribosomes, neurosecretory granules, and enzyme content of g-glutamyl transpeptidase, alkaline phosphatase, and aspartic transcarbamylase. The frozen lung is examined for its content of neurosecretory cells by fluorescence microscopy, and for alkaline phosphatase by classic histochemistry; fixed lung is diagnosed, its lesions scored by a multimode ordinal technic, and its population of mucus cells and tantalum-containing macrophages estimated. The apical or regulatory region of the bronchiole is further evaluated through collaboration with an experienced electron microscopist.

The above multidisciplinary design provides a description of some regenerative events in the bronchiole after irreversible injury, which is our first goal (item 6, p. 1). It also supplies clues to cellular alterations associated

100353864

Source: https://www.industrydocuments.ucsf.edu/docs/hgyh0000

with physiological alterations, our second goal, and some inferences for a predictive model of lung function after specific injury, our third goal. The design proposes no new methods, but rather an amalgamation of technics currently in use in two different research studies in our laboratory. Thus, all projected work loads are based on our own experience, particularly with advanced high-volume instrumentation.

(2) Details of experimental design:

a. Animals:

Purebred newborn strain II guinea pigs are from pedigree stock maintained and bred by us within our laboratory, in stainless steel Hoeltge cages, on Ralston Purina guinea pig chow ad lib. Temperature and humidity are continuously recorded by a Rustrak #255 dual channel strip chart; light, temperature, and human egress are controlled.

Individual cages of test and control animals are rotated on the rack at regular intervals according to a randomization procedure, in order to equalize all environmental and ecological effects, such as differential distribution of light, temperature, odor and noise. All animals are routinely subjected to bacteriological surveillance.

Newborn animals to be admitted to the protocol must weigh more than 80 g. and be healthy at birth. They must be the issue of dams at least four months old. Eligibility of dams for mating is judged by observation of the vaginal plug. Complete pedigree records are kept. Matings are scheduled.

10035386 42

Source: https://www.industrydocuments.ucsf.edu/docs/fhyl0000

b. Exposure to pulmonary irritant:

Oxygen exposure is carried out in a Labconco hood in flowing 100% or 60% oxygen according to our published method (7). The dose of oxygen is computed as hr%, viz. hours of exposure multiplied by the concentration of oxygen administered (29).

Smoke exposure is carried out according to a progressive scale of smoking, by which the daily frequency of exposure is increased, but the exposure period itself is constant (Fig. 4). Kentucky Standard Cigarettes, previously secured in large lots and stored under refrigeration, are smoked in a Walton positive pressure smoking machine secured under the auspices of Dr. J. H. Kreisher. The dose of cigarette smoke is calculated by the chlorinated hydrocarbon method of Alex Spears (to be published; personal communication J. H. Kreisher) with a chlorobiphenyl tracer compound. Controls "smoke" unlit cigarettes. The smoking schedule (Fig. 4) is tentative and subject to revision in accord with current experience. Cigarette dose is computed five ways: the total number of hours exposed, total length of cigarette smoked, total weight of cigarette smoked, and mean post-exposure hemoglobin: carboxyhemoglobin ratio estimated from spectrophotometric shift in the oxyhemoglobin Soret bands, and by Spear's tracer method.

In the standard smoking mode, the lit, measured, weighed cigarette is marked 2 mm from the hot tip and placed in the smoking machine and timed and observed. We anticipate development of Skinner-box experiments during the current NIH contract which will make acceptance of cigarettes a voluntary response of the animals but this is not a necessary part of the experimental design.

1003538643

FIG. 4

SCHEDULE OF EXPOSURE AND DOSE FOR
PULMONARY IRRITANTS: OXYGEN AND TOBACCO

AGENT	STRENGTH	WEEKS OF EXPOSURE 0 - 4	4 - 8	8 - 16
OXYGEN	HIGH DOSE (100%)	CONTINUOUS	--	--
	LOW DOSE (60%)	CONTINUOUS	CONTINUOUS	CONTINUOUS
CIGARETTE*	HIGH DOSE	1*	2	4
	LOW DOSE	1*	1	1

*1 numerical dose equals 3 mm cigarette smoked in 1 exposure

100353864

Source: https://www.industrydocuments.ucsf.edu/docs/hcyl0000

Diagram of Guinea Pig in Plethysmograph for Physiological Lung Function Studies

FIG. 8

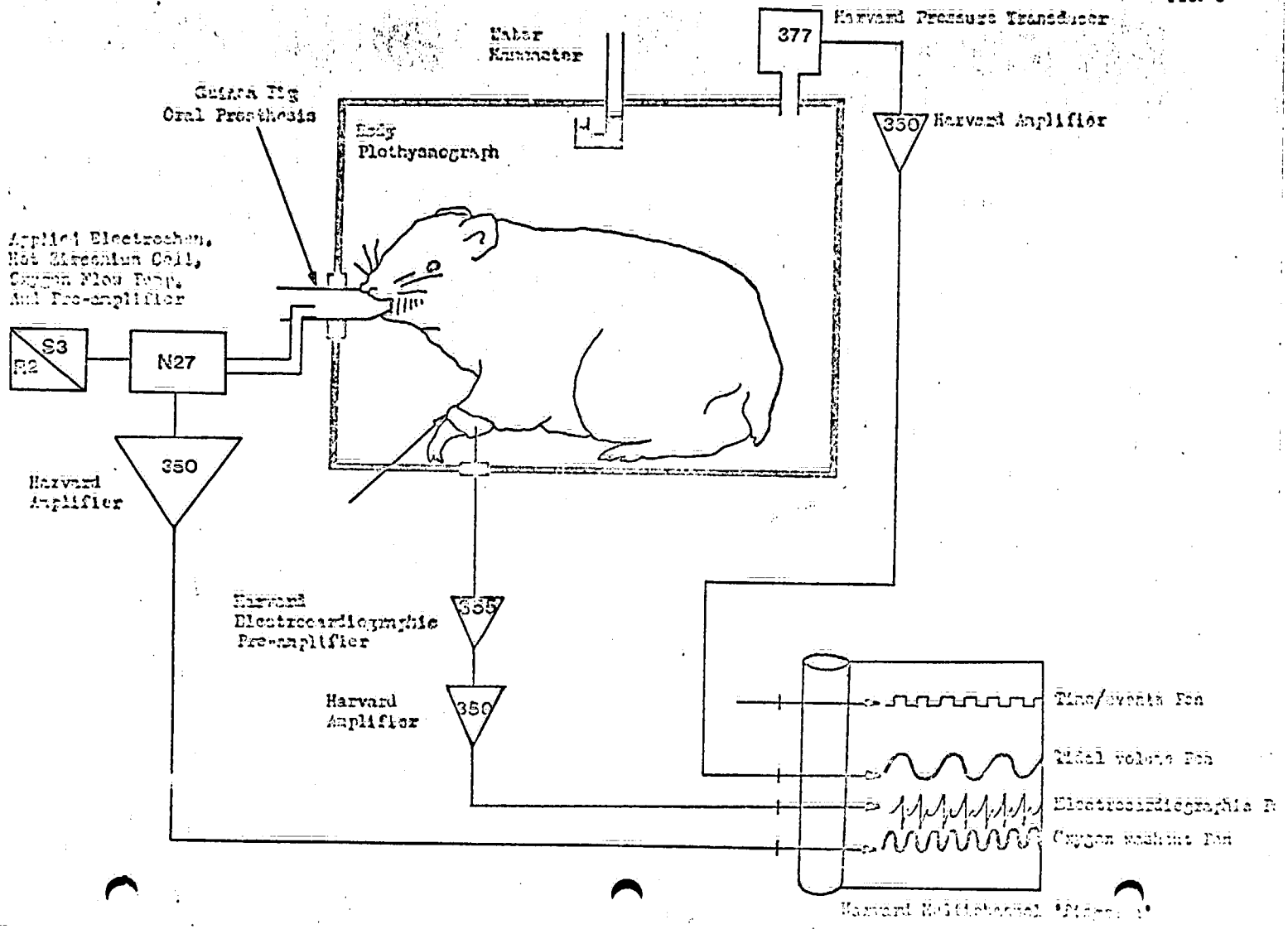

1003538645

Source: https://www.industrydocuments.ucsf.edu/docs/hqyl0000

c. Methods and materials: (FIGS. 9 & 10)

1. Clinical evaluation:

(a) Appearance: daily recorded check of coat, mouth, chest, abdomen, excreta; includes timed period for handling.

(b) Activity: daily recorded check of activity, posture, gait, and response to standard non-conditioned stress.

(c) Weight: Ohaus animal balance (±0.1 g.) daily.

(d) Rectal temperature: Yellow Springs Instrument amplifier #43TA, and probe #402 (±0.1° C) thrice weekly.

(e) Hemogram: red cell count, hemoglobin, hematocrit, computed indices, and white cell count by Coulter S; differential smear by Romanowsky stain, weekly.

2. Serum chemistry (biweekly):

(a) Alkaline phosphatase: isoenzyme estimation from gel acrylamide electrophoresis, modified from the method of Gluck by us (30, 31, 32), and performed for total serum enzyme by automated replicate technic in Abbott ABA 100A analyzer. This instrument is explained and depicted in Fig. 11 A & B, and the machine method has been adapted by us from a "Sigma" kit.

(b) G-Glutamyl transpeptidase: total enzyme estimation by the p-nitroanilide method of Orlowski (33, 34) according to the formula: 2 g-glutamyl-p-nitroanilide + g-glutamyl transpeptidase ⟶ (g-glutamyl)(g-glutamyl)-p-nitroanilide + p-nitroaniline; method is modified by us for replicate estimation on the Abbott 100A analyzer (35). A "Dade" kit is used.

(c) Aspartic transcarbamylase: total enzyme method of Porter, Modebe, and Stark (36), as modified by Normal Kretchmer and Nicholas Hoogenraad (personal communication). In this method,

10035386

Source: https://www.industrydocuments.ucsf.edu/docs/

SCHEDULES OF TYPES OF IN VIVO EXAMINATION FIG. 9

EXAMINATION	TESTS PERFORMED	WHEN PERFORMED				
		FIRST DAY OF LIFE	THRICE WEEKLY	BI-WEEKLY		AT TERMINATION
				IN PLETHYSMOGRAPH	NOT IN PLETHYSMOGRAPH	
PHYSIOLOGICAL LUNG FUNCTION EVALUATION	PO_2 PCO_2 pH Minute ventilation Nitrogen washout			+		
CLINICAL EVALUATION	Appearance Weight Ventilatory rate Pulse Temperature	+	+			+
CLINICAL LABORATORY EVALUATION OF BLOOD	Hemoglobin/hematocrit Red cell indices Leucocyte count Differential smear Carbon monoxide Aspartyl transcarbamylase Glutamyl transpeptidase Isozymal alkaline phosphatase	+			+	
TISSUE PATHOLOGY EVALUATION*	Subgross giant section Histologic grades 3 enzymes (above) Neurosecretory granules Goblet cell count Tantalum macrophage count					+

*Note: electron microscopy on selected specimens only, based on tissue pathology evaluation.

22

1003538647

Source: https://www.industrydocuments.ucsf.edu/docs/hqyl0000

FLOW DIAGRAM OF BI-WEEKLY PHYSIOLOGICAL LUNG FUNCTION TESTS

WITH ALLOCATIONS OF EQUIPMENT AND PERSONNEL

TEST DATA	STEADY STATE 10 min	COLLECT DATA PERIOD	INHALES 100% O_2 5 min	COLLECT DATA PERIOD	STEADY STATE 10 min	METHOD AND EQUIPMENT	PERSONNEL
SINGLE LEAD ELECTROCARDIOGRAM	+	+	+	+	+	Electronic amplification of pulse, respiration, minute ventilation; Harvard Apparatus Co. amplifiers, transducers, multichannel chart.	Technician #1 (physiologist)
VENTILATORY RATE	+	+	+	+	+		
MINUTE VENTILATION		+					
NITROGEN WASHOUT (pulmonary mixing)		+		+		High temperature electrochemical cell plus above; Applied Electrochemistry Co. instrument.	
P_AO_2		+		+		Micro-electrode digital mobile blood gas station; Corning 165C analyzer.	Technician #2 (clinical chemist)
P_ACO_2		+		+			
pH		+		+			
CARBON MONOXIDE		+				Scanning 2-wavelength Spectrophotometry; Perkin-Elmer 124	

10035386 48

Source: https://www.industrydocuments.ucsf.edu/docs/hqyl0000

FIG. 11 A

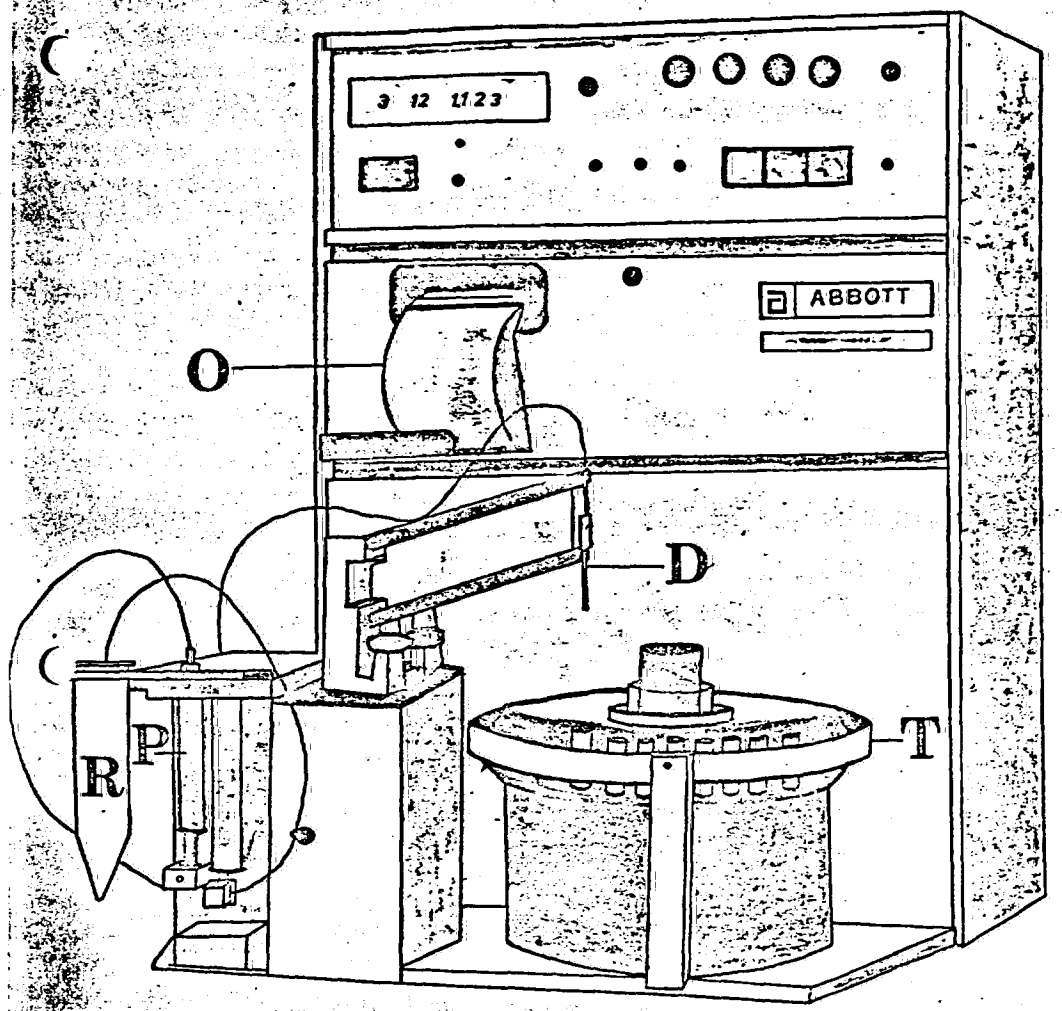

O = Output on tape of true kinetic data

D = Dipping needle on arm to introduce reaction mixture and transfer samples

R = Reservoir for reaction mixture

P = Pump syringe for dispensing reaction mixture automatically

T = Turntable with sample tubes in outer ring, cuvettes in middle ring (not shown) and 2-wavelength spectrometer in center (not shown)

This is the only two-wavelength automated enzyme analysis system available, and has been in use for the last four months. The particular advantage is the much greater accuracy and precision over a much wider range (see Fig. 11 B). See reference #35.

10035386 49

Source: https://www.industrydocuments.ucsf.edu/docs/hqyl0000

NADH

FIG. 11 B

SAMPLES INTRODUCED MANUALLY

Two-wavelength enzyme measuring technic. Standard deviations are acceptable even when enzymatic activity is measured at very high optical density. This makes the instrument especially useful for research investigations in which the order-of-magnitude concentration of the sought for enzyme has not been established or is completely unknown.

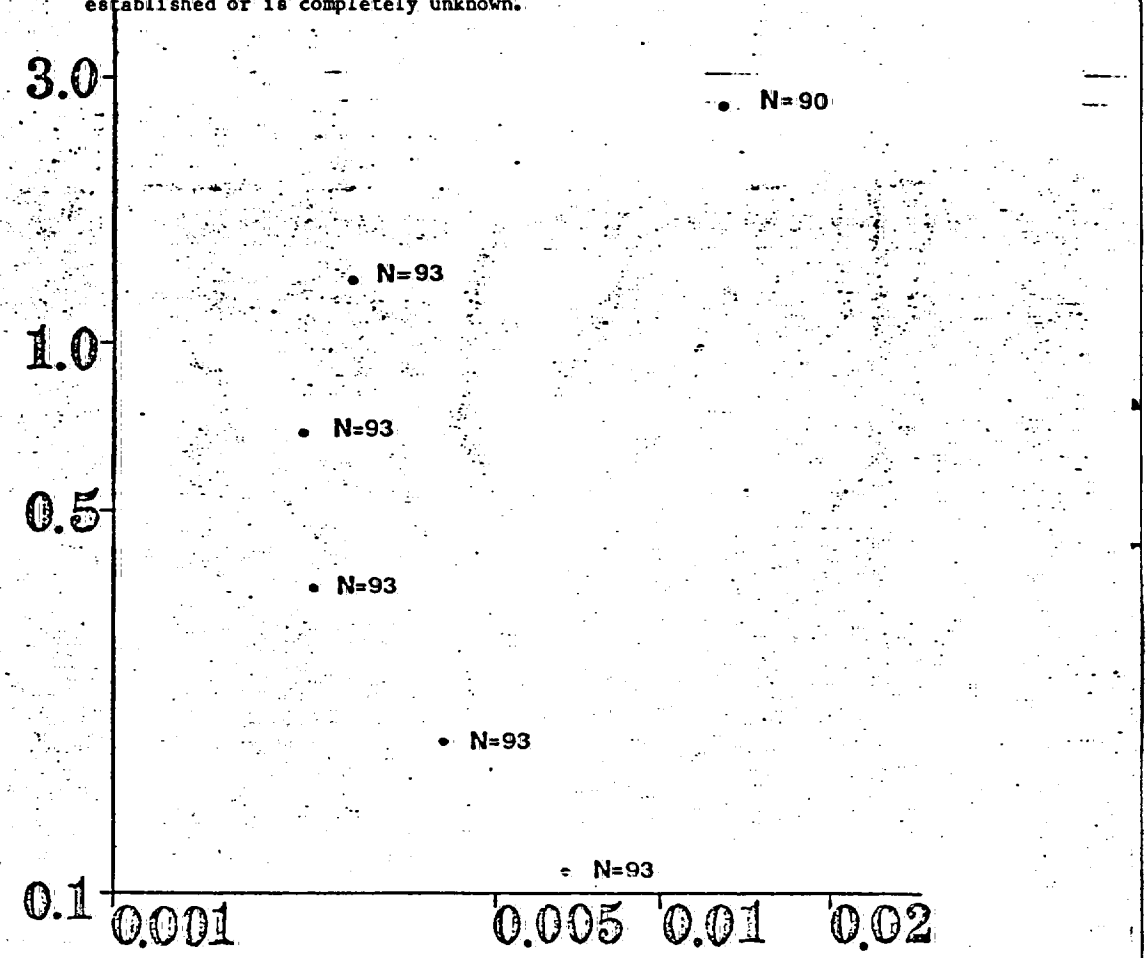

10035386S0

Source: https://www.industrydocuments.ucsf.edu/docs/hgw0000

^{14}C-L-Aspartate is the substrate; the product of enzymatic activity, ^{14}C-carbamylaspartate, is generated by interaction with carbamyl phosphate. Then, the product is isolated on Dowex 50 ion exchange resin (H^+ form) and eluted with buffer:

$$\text{Car-P} + {}^{14}\text{C-Asp} + \text{aspartic transcarbamylase} \longrightarrow \text{Car}({}^{14}\text{C-Asp}) + \text{P}.$$

The reaction is carried out for 15 minutes at 37°C after a 1-minute preincubation, and ended by precipitating enzyme with trichloracetic acid. We count it on a Nuclear Chicago Unilux II, with computations carried out on a Hewlett Packard 9800 microcomputer.

(To our knowledge, this is the first proposal to evaluate the presence of aspartic transcarbamylase in serum except for our own current NIH contract work. The importance is that, unlike all common clinical tests of serum enzyme activity, that for aspartic transcarbamylase evaluates the presence of an enzyme specific and obligate for the synthesis of DNA during mammalian cell replication. Thus, presence of aspartic transcarbamylase in serum in increased amounts is a definitive marker for regenerative nuclear activity, whereas all other enzymes in clinical analysis are markers for injured or regenerating cytoplasmic systems, or increased cell membrane permeability.)

(d) Blood gases:

These are established from capillary blood samples, by the use of a Corning 165C blood gas station. This machine computes PO_2, PCO_2, (HCO_3^-), and pH from 100 µl samples, which we plan

1003538651

Source: https://www.industrydocuments.ucsf.edu/docs/mpjl0000

on a biweekly schedule. The use of "arterialized" capillary gases has received extensive comment in human literature on neonates; briefly, the method is valid but in establishing relative rather than absolute values. The machine and technic are in routine use in our current studies, and normal values have been established for strain II guinea pigs, by us.

(3) Pulmonary function studies (biweekly):

Under the current NIH contract, a complete ventilation station has been constructed and is in use and it is this which we shall utilize. The station is based upon a body plethysmograph designed by us specifically for studying guinea pigs, together with a novel mouthpiece which we design and produce from casts of the guinea pig's oral cavity (Fig. 5,6,7) Thus, the animal is snugly confined within the plethysmograph by a bulky restraint, and the tightly fitted mouthpiece protrudes through a gas-tight port. A Harvard Biograph #2120 5-channel strip chart simultaneously records pulse, respirations, tidal exchange, and pulmonary mixing, as explained below. (The fifth channel is a time-and-events pen.)

a. Pulse is recorded by a single lead electrocardiograph.

b. Respirations are recorded with a pneumotachygraph.

c. Tidal exchange is measured with a Harvard #377 pressure transducer.

d. Pulmonary mixing:

Nitrogen washout is measured by a novel method. As usual (37), the animal is subjected to 100% oxygen for 5 minutes. Then, by multiple-breath open-circuit technic, the change in P_AN_2, after cessation of 100% oxygen, is analyzed by means of a rapid-action hot zirconium cell.

10035386S2

Source: https://www.industrydocuments.ucsf.edu/docs/fnyf0000

However, the innovation is that the cell actually measures P_AO_2 which, in the absence of marked CO_2 retention, is an accurate reciprocal measure of P_AN_2 when the vapor tension of water is constant: $P_AO_2 \sim 760 - (P_AH_2O + P_ACO_2)$ when $P_AN_2 \rightarrow 0$. The method makes use of the fact that fast action (c. 35 msec) oxygen cells of quite low dead space (c. 200 µl) are available in clinically useful form, e.g. Allied Electrochemistry #S-3/R-1/N-22M (Fig. 8).

(The basic assumptions for use are tenable: by the time CO_2 retention occurs, the physiological demonstration of uneven ventilation is redundant in these experiments; and the alveolar vapor tension of water is rarely subject to significant change in any event. The frequency response of the Harvard Biograph, in excess of 100 Hz, is sufficient to handle the graphic output; and there is also available a Hewlett Packard 7400 A X-Y recorder for more linear output at a slewing speed in excess of 250 cm/sec. This method is in routine use in our NIH contract work.)(Fig. 27)

e. Minute ventilation:

This is computed by calibration of the displacement of the Harvard pressure transducer used with the body plethysmograph (Fig. 8) and then integration of the resultant strip chart readings with respect to the areas under the curve. Whether the test animal is in steady state may in part be confirmed from the simultaneous electrocardiograph and breathing frequency records. The period of observation is such that, excluding sighs, all the observed results are statistically linear (flat) with time.

100353865

Source: https://www.industrydocuments.ucsf.edu/docs/[illegible]

(4) Chest Roentgenography:

a. The technic is essentially that we have published before (7) except that it is now possible to get improved resolution with the use of Siemens tube with an 0.9 mm focal spot, instead of the former 2 mm size. The beam is used unfiltered at 850 ma, 40 KV, 1/125 sec, at a precisely constant distance of approximately 65 cm; Kodak type AA film or the equivalent is used with par-speed screens, and developed in a high speed Picker automatic hot processor. The animals are immobilized in a plastic rack during roentgenography.

b. Tantalum powder bronchography:

The technic is that of Nadel, Wolfe and Graf (6); the basis is the radio-opacity of aerosolized tantalum powder, combined with its availability in tightly controlled particle size, and its relatively banal non-toxic behavior in all human and animal experiments to date. This technic is also part of our current N.I.H. Contract routine. In use, accurately measured weights of dry tantalum powder of 10 μ particle size are dispensed into a small chamber equipped with a recirculating Muffin fan. The test animal is placed within the body plethysmograph (Fig. 8) and connected by means of his oral prosthesis to the tantalum powder chamber. He breathes powder by closed circuit technic for precisely 1.0 minutes during which time his minute ventilation and tidal volume is recorded. Six hours (± 1) and 48 hours (± 6) later, he is roentgenographed by the described technic. Directly thereafter, at a recorded time, he is sacrificed and autopsied.

100353865

Source: https://www.industrydocuments.ucsf.edu/docs/hqg0000

(5) Autopsy procedures:

a. General necropsy: The details are shown in Fig. 12-14. In brief, all organs except the brain are dissected and examined; the major viscera are weighed, and specific notations are entered as shown. The animals are despatched by a blow to the skull; the lungs are rapidly dissected, weighed, and volume measured by displacement, so that material for electron microscopy and molecular dissection is available within 30 seconds and well preserved. After, there is a more leisurely gross examination of the remainder of the specimens.

b. Heart: The heart is weighed and examined, and the anterior right ventricular wall, posterior left ventricular wall, and intraventricular septum are separately dissected and weighed. The objective is to evaluate possible right ventricular hypertrophy in the light of functional and histological lung lesions (Fig. 12).

c. Lungs: The weight and displacement are recorded (above). Then, three types of samples are recovered from three standard loci, as follows. A 1-mm block of the full lung, from apex to base, and through the hilum is removed in the lateral plane. This block is the source for all anatomical material; the remainder, or the bulk of the lung tissue, is for molecular dissection (see below). Of this block, the right middle lobe is arbitrarily the source of all material for electron microscopy, alkaline phosphatase histochemistry, and secondary fluorescence of neurosecretory granules; the last two evaluations are performed with material frozen at -170°C. Details of these methods are given below. In addition, 5 μ and 50 u sections are prepared from regular paraffin-embedded material of upper and lower lobes.

1003538655

Source: https://www.industrydocuments.ucsf.edu/docs/[illegible]

FIG. 12

FLOW DIAGRAM OF AUTOPSY AND MICROSCOPY PROCEDURES

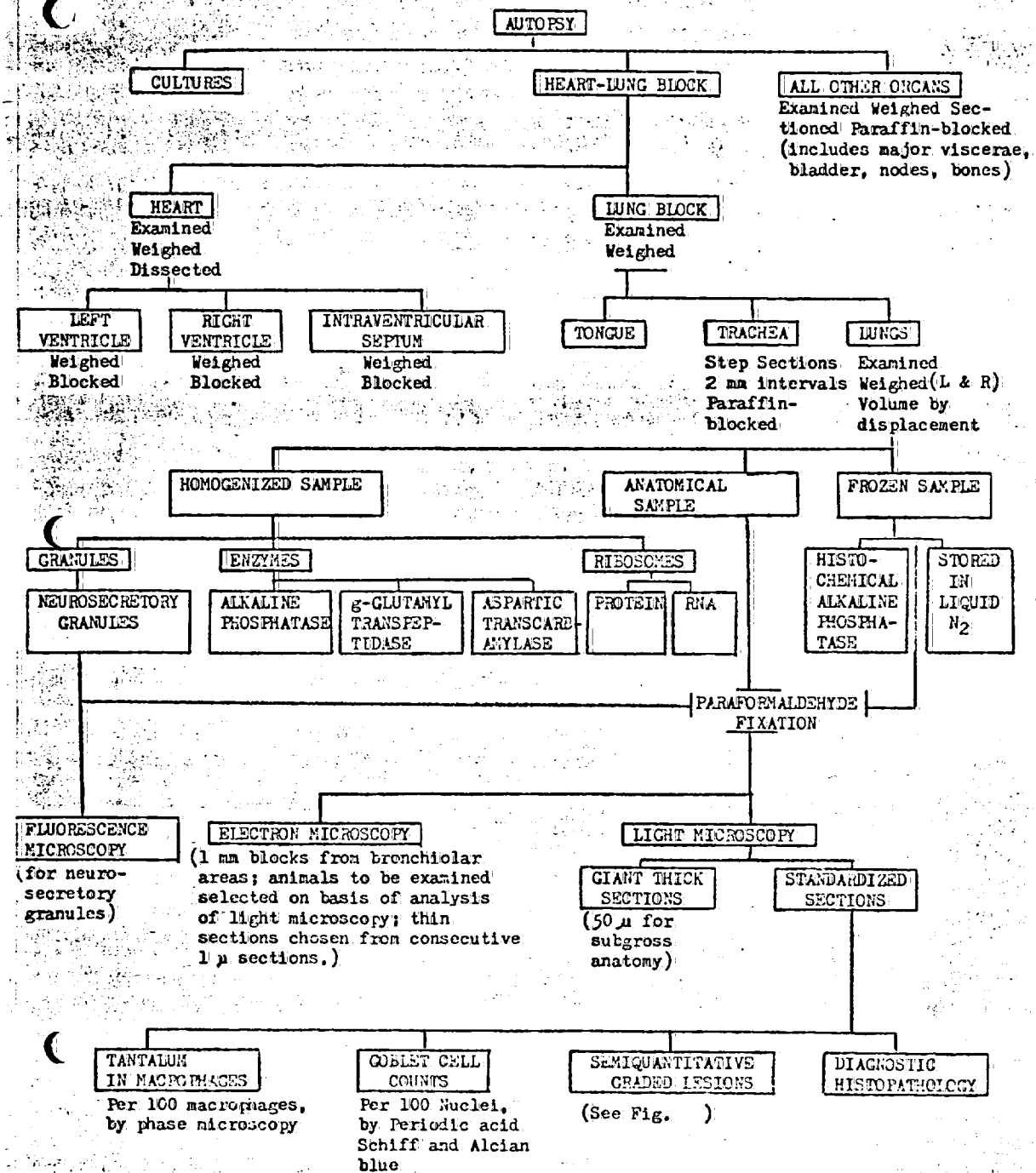

100538656

Source: https://www.industrydocuments.ucsf.edu/docs/hgyl0000

FIG. 13 A

AUTOPSY INFORMATION CHECK LIST (PART 1)

REPORT # _____

ANIMAL IDENTIFICATION: _____
DATE: _____
TIME: _____
PROSECTOR: _____

FIXATIVE: HCHO: ____
PARA: ____
GLUT: ____
OTHER: ____

GENEOLOGY: _____
PICTURES: _____
FROZEN: _____

AGE: _____days
SEX: M F
WEIGHT: _____g
LENGTH:
NOSE-RUMP: _____cm
NOSE-TOES: _____cm
CHEST: _____cm

COAT: _____
HEAD: _____
BREASTS: _____
UMBILICUS: _____
GENITALIA: _____
LIMBS: _____

PLEURAL CAVITY:

PERICARDIAL CAVITY:

MEDIASTINUM:

ABDOMEN:

RETROPERITONEUM:

REMARKS:

1003538657

Source: https://www.industrydocuments.ucsf.edu/docs/[illegible]

FIG. 13 B

DETAILED SYSTEMIC EXAMINATION (PART 2)

REPORT #_____

SYSTEM	ORGAN	WEIGHT	DIAGNOSIS GROSS	DIAGNOSIS MICROSCOPIC	OTHER/ADDITIONAL
VENTILATORY	TONGUE	-	-	+	
	TRACHEA	-	-	+	PAS- Alcian Blue
	CARINA	-	-	+	PAS- Alcian Blue
	LUNG	R L	+	See Fig.	PAS- Alcian Blue Elastic Van Giesen
	DIAPHRAGM	-	-	+	
CARDIO-VASCULAR	HEART	R. Vent L. Vent I-V Septum	+	+	
	GREAT VESSELS	-	-	+	Elastic Van Giesen
URINARY	KIDNEY	+	+	+	
	BLADDER	-	+	+	
LYMPHO-RETICULAR	SPLEEN	+	+	+	Giemsa
	NODES	-	+	+	
	THYMUS	+	+	+	
	PEYER PATCHES	-	-	+	
	BONE MARROW	-	-	+	Giemsa
GASTRO-INTESTINAL	ESOPHAGUS	-	-	+	
	STOMACH	-	-	+	
	DUODENUM	-	-	+	Single Specimen
	JEJUNUM	-	-	+	
	ILEUM-CECUM	-	-	+	
	COLON	-	-	+	Single Specimen
	LIVER	-	-	+	
	PANCREAS	-	-	+	
ENDOCRINE-GONADAL	PITUITARY	-	-	+	PAS- Orange G
	THYROID	-	-	+	
	PARATHYROID	-	-	+	
	ADRENAL	+	-	+	
	GONADS	+	-	+	
	UTERUS/ VESICLES	+	-	+	

1003538658

Source: https://www.industrydocuments.ucsf.edu/docs/hgyd0000

ORDINAL GRADES OF LUNG LESIONS FIG. 14

CATEGORY	GRADE 0 (NORMAL)	GRADE I (REACTION)	GRADE II (NECROSIS)	GRADE III (REGENERATION)	GRADE IV (CHRONICITY)
BRONCHIOLAR MUCOSA	normal	> 25% of cells necrobiotic or exfoliating	> 50% of cells necrotic	> 25% of cells atypical or metaplastic	plus hyperplasia
ARTERIOLES	normal	edema of muscle	muscular proliferation	plus intimal proliferation	plus periarteriolar infiltrate
LYMPHATICS	normal	dilated	severely dilated	perilymphatic infiltration	perilymphatic fibrosis
GOBLET CELLS	normal	25% increase	50% increase	100% increase	100% increase
HYALINE MEMBRANES AND/OR EDEMA	absent	10-50% of air sacs	50-100% of air sacs	plus 10-50% of bronchioles	plus 50-100% of bronchioles
INFLATION PATTERN	normal	> 25% alveolar atelectasis	> 25% lobular or lobar atelectasis	plus lobular distention	plus lobular emphysema
ALVEOLAR INTERSTITIUM	normal	edema	focal fibroplasia	diffuse fibroplasia	plus fibrosis
ALVEOLAR INFLAMMATORY REACTION	neutrophiles absent	5% air spaces with neutrophiles	33% air spaces with neutrophiles	foci of pus	neutrophiles and plasma cells
	macrophages	5% air spaces with free macrophages	33% air spaces with free macrophages	macrophage plugs in airways	macrophage proliferation filling lobule
HEMORRHAGE	absent	10-50% of alveoli	50-100% of alveoli	plus extension into bronchioles	plus interstitial in 2 or more major septae

100353859

Source: https://www.industrydocuments.ucsf.edu/docs/hqyl0000

The 5 μ sections are evaluated double-blind in four ways: routine histopathological diagnosis, ordinal grades of specific lesions (Fig. 12), estimation and location of tantalum-containing macrophages, based on phase microscopy; and a sensitive fluorescent periodic acid Schiff and Alcian blue routine, previously used by us (38) and adapted to the small mucosal cells of normal guinea pigs. Details of this methodology are also given below.

1. Electron microscopy: This is carried out on 1 mm blocks which have previously been identified as primarily bronchiolar in fresh material under the dissecting microscope at necropsy according to our published methods (29). The pH is controlled in order to maximize standardization of observation for neurosecretory granules (39); after we embed it in Epon, the material is stained by osmification at controlled pH (40). The objective of the microscopist is to provide 15 publishable pictures documenting the cellular changes and alterations in neurosecretory granules when irreversible injury is compared to the control. Therefore, "thin" sections will be selected by decisions reached after the visualization of juxtaposed "thick" sections in phase, light, and fluorescence (41) microscopy.

2. Alkaline phosphatase histochemistry: This is carried on frozen sections post-fixed in paraformaldehyde, with the classic naphthol AS-MX coupling technic at pH 8.6 in the presence of $MnCl_2$ (42); reagents are from a 'Sigma' kit, and the counterstain is Mayer's hematoxylin. The objective of this test is to determine the cellular sources of enzyme isolated on the ultracentrifuge (below) as well as to provide information about the differentiation of mucosal and endothelial cells before, during, and after irreversible injury. This is also the enzyme of our choice

1003538660

Source: https://www.industrydocuments.ucsf.edu/docs/kqvl0000

with which to begin future ultrastructural studies of specific microsomal protein production after irreversible injury, inasmuch as the cyto-enzyme technic has been frequently published from other laboratories, and we have a well-tried method available (43) which has been modified for optimal performance (Bengt Robertson, personal communication).

3. Neurosecretory granules: The active material in pulmonary Kultschitsky cells is not known, but is universally assumed to be enterochromaffin and neurosecretory in nature; these cells are included by Pearse in the so-called APUD family of amine and kinin secreting cells (44). It is well accepted that active granules fluoresce upon reaction with small aldehyde molecules; typically, dopamine, noradrenaline, or 5-hydroxytryptamine is reacted with formaldehyde, paraformaldehyde, or glutaraldehyde. The reaction, not well understood, has been discussed by Corrodi (45). We have chose a modification worked out in the laboratory of our close collaborator, J. M. Lauweryns (46).

At necropsy, 1-mm lung blocks from standard areas (see Fig. 12) are plunged into isopentane at at -170°C in liquid nitrogen, and then freeze-dried with a Virtis cold trap and a Cenco vacuum pump. The dry material is reacted with formaldehyde generated from paraformaldehyde at a relative humidity of 60% ± 10, by the use of concentrated sulfuric acid, and exposure of the sections to the vapor in a closed chamber is accomplished for one hour at 80°C. This develops fluorescence of dopamine, 5-hydroxytryptamine, and noradrenaline; an additional two hours develops adrenaline (47). The sections are mounted in polyester wax and flouresced with an Osram HB 200 mercury lamp at about 404 nm with a BG 12 filter, and observed above 520 nm under darkfield conditions with barrier filters Schott GG-9 and OG-1. Results are checked by phase microscopy and by silver staining (argyrophilia); controls are checked by the borohydride method (45).

1003538661

Source: https://www.industrydocuments.ucsf.edu/docs/hqyl0000

4. Ordinal grades for semiquantitative evaluation of lesions:

This method is based on our previous observations of oxygen-induced rat bronchiolar lesions (48), which have been confirmed by similar ordinal grading of guinea pig, (7) mouse (49), and human infant (21) lungs after oxygen intoxication. The table of ordinal grades is shown (Fig.14); in the method, hematoxylin-eosin stained paraffin sections of entire lung in the mid-lateral plane then are evaluated double-blind.

5. Goblet cell counts:

The major innovation is is that the goblet cells are counted by a fluorescent rather than a visible periodic acid Schiff reaction, by the substitution of acriflavine for the more common Schiff's fuchsin; the remainder of the reaction is classical. (5) . We have previously used this technic in paraffin and plastic embedded specimens. (5) . The reason for the fluorescence application is that bronchiolar goblet cells of guinea pigs are often quite difficult to visualize in ordinary light technic. In order to count goblet cells per 100 nuclei, a nuclear stain of Alcian blue at pH 2.8 is useful, since it not only stains nuclei quite well by fluorescence (R. C. Rosan, unpublished) but gives additional clues to the type of glycoprotein in bronchiolar glyocalyx and in the mucus-producing apparatus (3). The fluorescence equipment and optical conditions are the same as for neurosecretory granules (above). By double blind technic, all goblet cells in the entire section of whole lung in the mid-lateral plane are counted.

6. Tantalum particle macrophage counts:

The same sections used above are re-examined for tantalum-containing macrophages by phase microscopy. The total number of macrophages

10035386 62

Source: https://www.industrydocuments.ucsf.edu/docs/hqp10000

is also counted, and a ratio established. In the event the macrophages are two numerous to count, i.e. over 1000 present in an entire section, sample areas will be examined by a randomization technic. The macrophage counts will also be related to the total number of airways per section. The tantalum content of each cell counted will be estimated in four ordinal grades: (0) no observable particles; (1) less than 5 particles (2) less than 50 particles (3) more than 50 particles.

7. Ordinary histopathologic diagnosis:

This is the usual diagnostic technic by which pneumonitis, chronic fibrosis, and other possible lesions may be classified. However, we do not propose to use or investigate the term emphysema in this proposal; instead, purely descriptive terms will be used (e.g. centrolobular bronchiolar atrophy, alveolar septal atrophy, etc.).

100538663

Source: https://www.industrydocuments.ucsf.edu/docs/hqyf0000

There exist tabulated times and gradient volumes for a B-14 zonal rotor, which we shall adapt and use; they give figures for Euglena spp. and E. coli ribosomes, which are quite close in physical characteristics to human ones (54).

The non-linear gradients are formed with a pre-programmed ISCO dialagrad #380 pump, and the rotor is unloaded with additional 2M sucrose solution, so that the effluent is directed through a 2-channel recorder (see a. 1. above) to a fractionator as before. However, the resolution is greatly increased, approximately 3-8x by zonal technic. Also, this rotor effects a great savings in labor due to its much higher capacity. This permits up to 10 animal experiments to be pooled (and thus averaged) in a single batch.

1003538664

Source: https://www.industrydocuments.ucsf.edu/docs/bqyx0000

FIG. 15

LUNG MICROSOMES

RABBIT AND GUINEA PIG

5-20% SUCROSE GRADIENT
MICROSOMAL PREPARATION + 0.5% BRIJ
GUINEA PIG AND RABBIT (1 g)
GLUCK METHOD

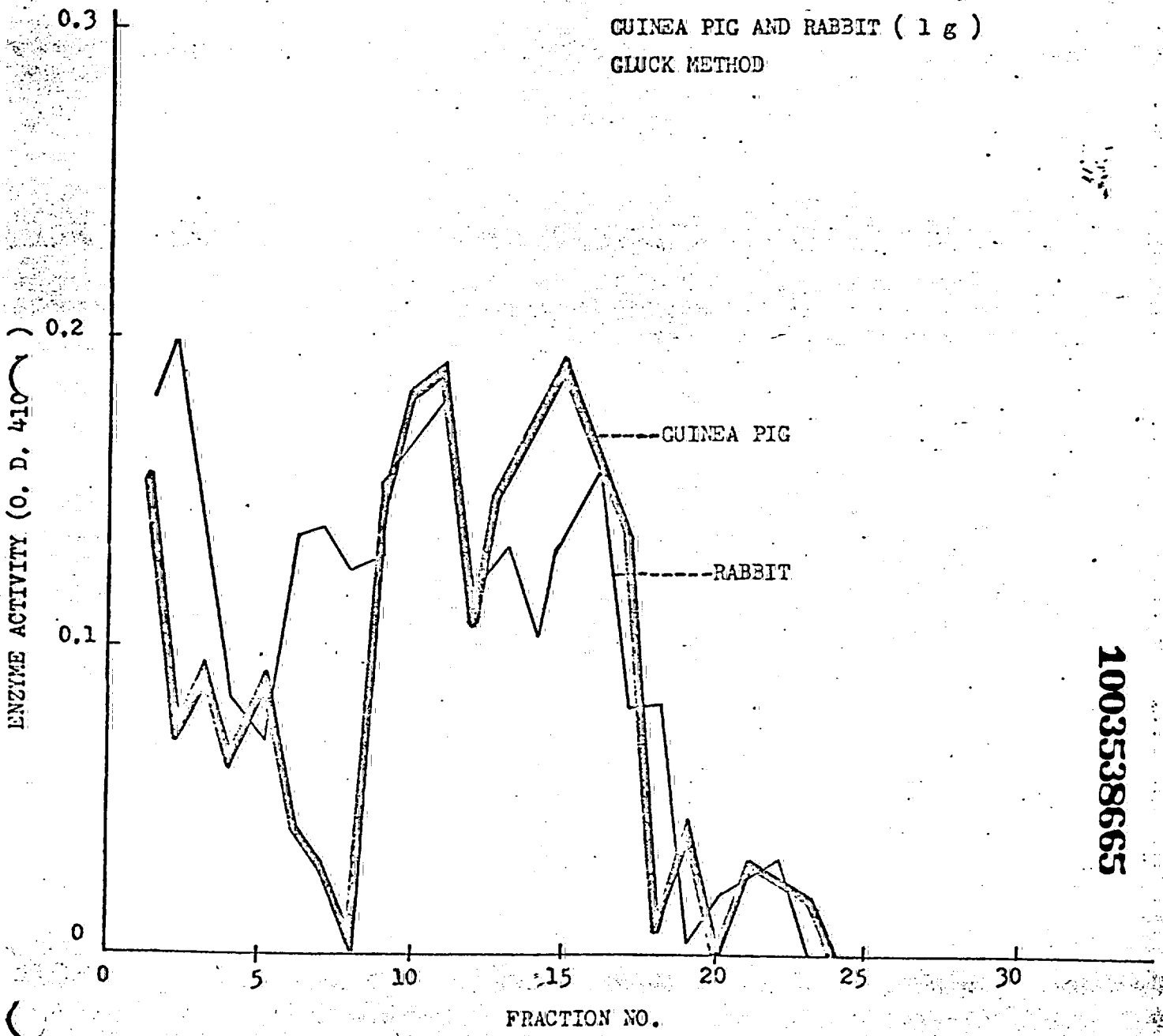

100353865

Source: https://www.industrydocuments.ucsf.edu/docs/hqyl0080

FIG. 16

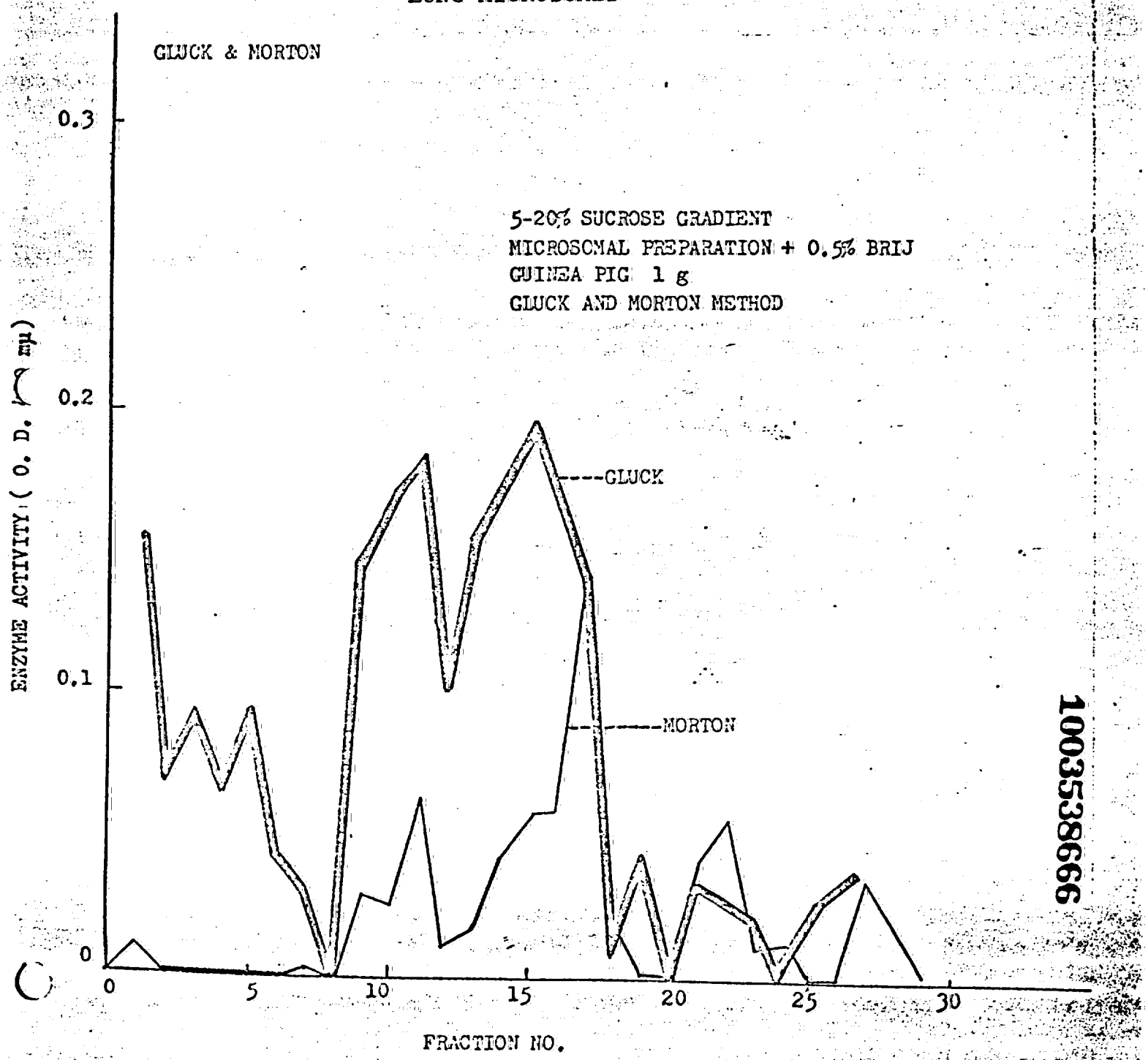

1003538666

Source: https://www.industrydocuments.ucsf.edu/docs/hqyl0000

FIG. 17

(42)

UNBORN (CANALICULAR) MEAN WEIGHT ~ 40 GRAMS

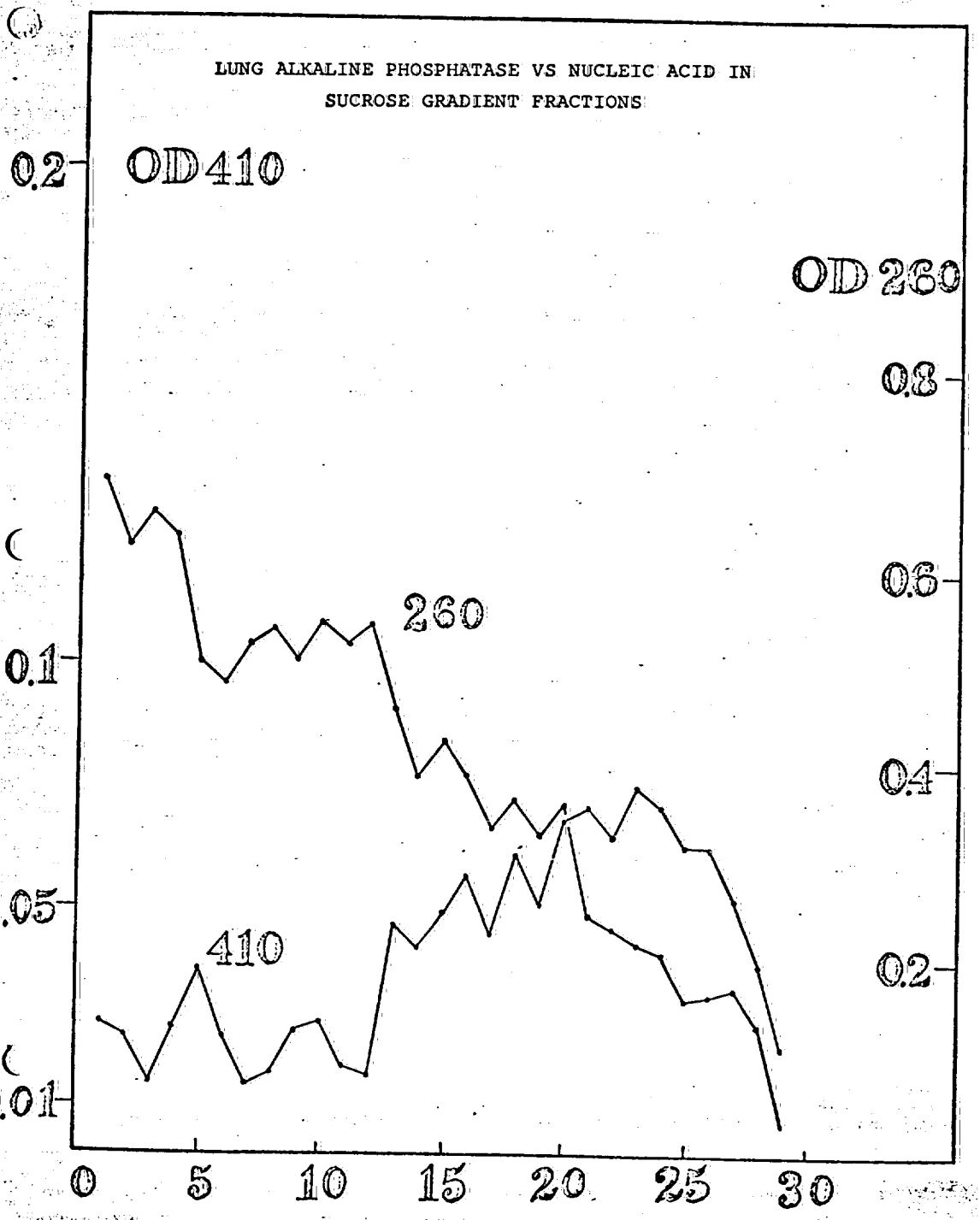

1003538692

Source: https://www.industrydocuments.ucsf.edu/docs/hgyl0000

FIG. 18

NEWBORN (SACCULAR)
MEAN WEIGHT ~ 55 GRAMS

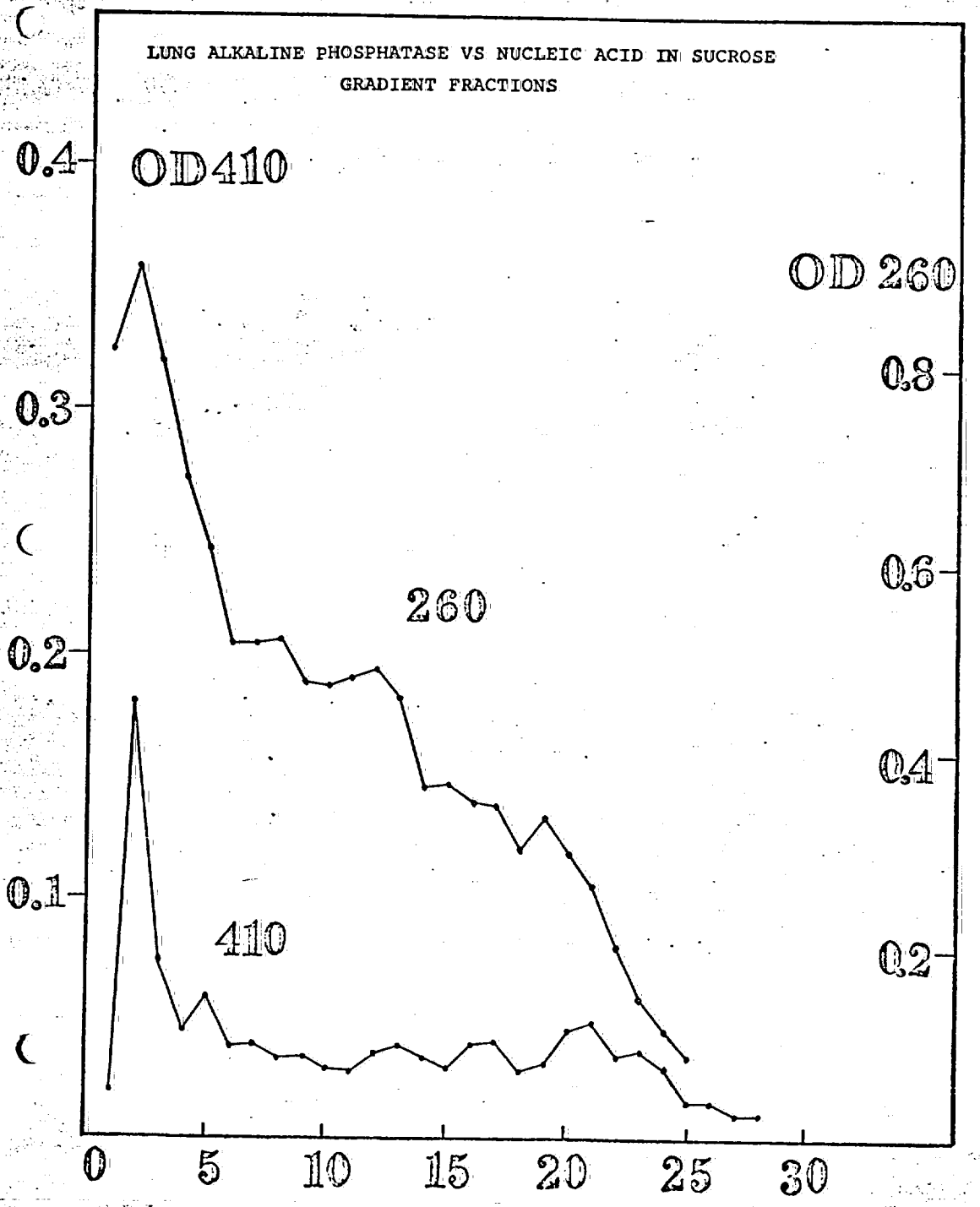

1003538668

Source: https://www.industrydocuments.ucsf.edu/docs/hqvl0000

FIG. 19 (44)

ADULT (ALVEOLAR)
MEAN WEIGHT ~ 835 GRAMS

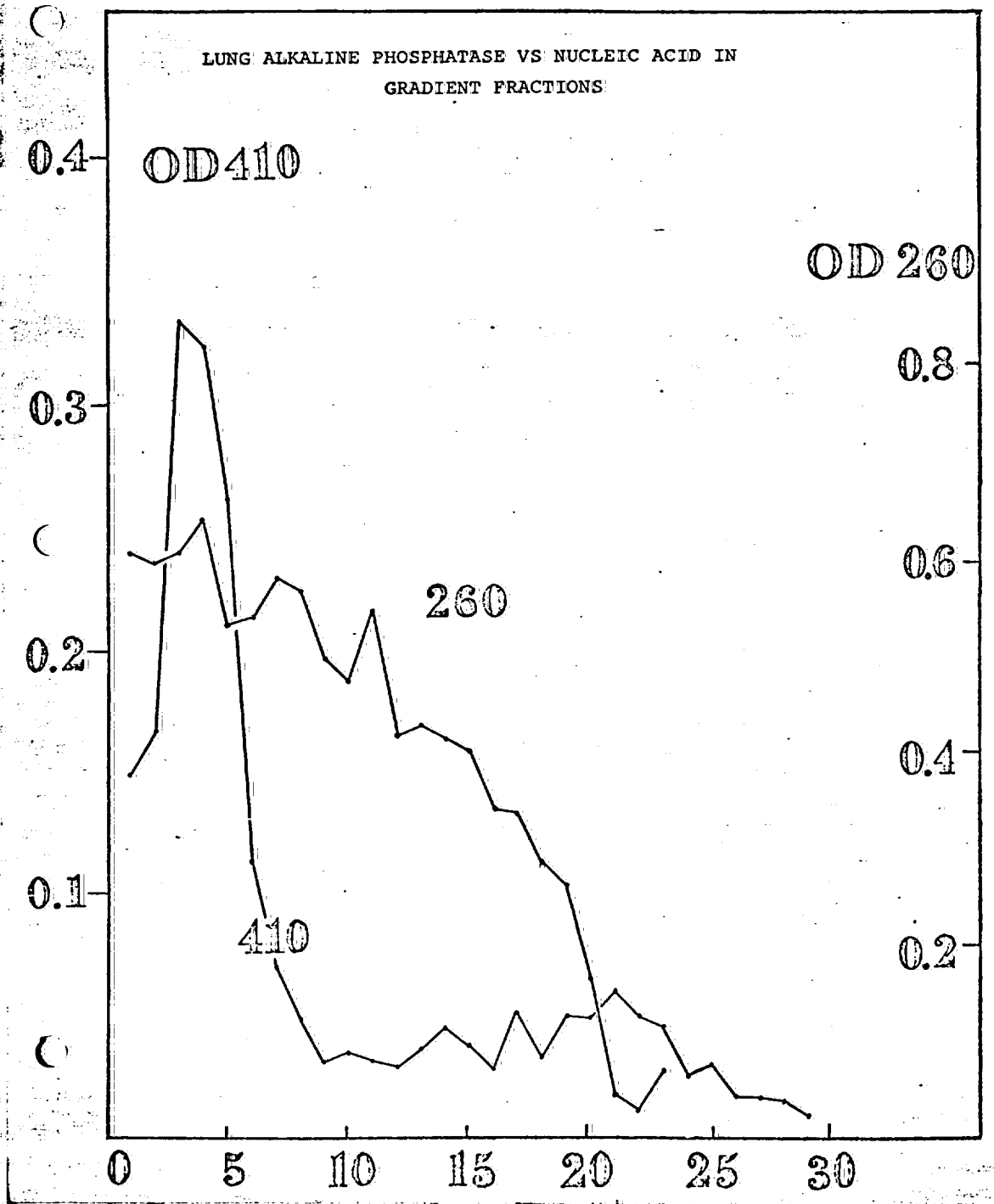

100353869

Source: https://www.industrydocuments.ucsf.edu/docs/hgv0000

FIG. 20 45

JUVENILE (ALVEOLAR)
MEAN WEIGHT ~ 500 GRAMS

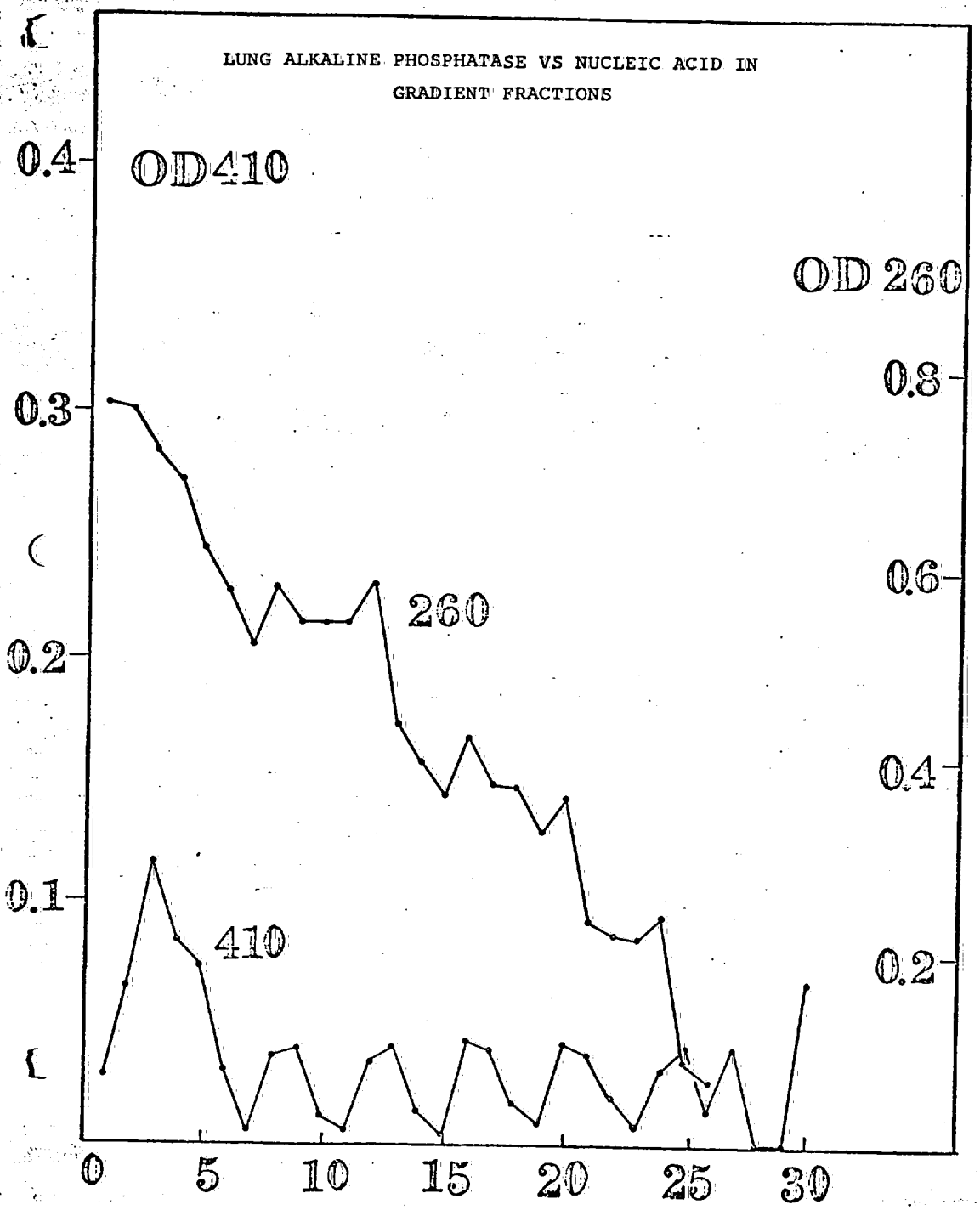

10035386?0

Source: https://www.industrydocuments.ucsf.edu/docs/hqyf0000

(d) Lung homogenates:

All procedures are based on the reduction of bulk lung tissue to a single homogenate (see item (5) c. above), which is then subjected to ultracentrifugation. The high speed fraction, which contains microsomes, ribosomes (3,50), small vesicles, and neurosecretory granules (51), is then analyzed by appropriate study of fractions prepared from sucrose gradients.

1. General method of fraction preparation Fig. 29.

a. The method and its modifications have been previously published from our laboratory (3,50,52,53). (This is not the method of choice, but is the backup method for zonal ultracentrifugation, see below. However, numerous mechanical and instrumental misadventures (none of them due to the technic of our laboratory) have kept our zonal rotor out of service approximately 78% of working hours in the past 18 months. Therefore, while we prefer to carry out the experiment outlined on the zonal rotor, and while numerous other investigators have achieved similar or more demanding analytical separations, we are no longer sanguine that a complete study may be planned about the zonal method alone.)

The lungs are flushed through the pulmonary artery in situ with Ringer's solution (pH 7.4, 0°C), immediately resected, and minced with razor blades. The mince is forced through an hydraulic press (Carver Company) at 2000 psi, and the resultant "brei" is strained through cotton gauze to remove gross lipid. The "brei" is homogenized in a Teflon pestle in buffer-detergent (0.0015M $MgCl_2$, 0.01M KCl, 0.001M 'Tris', 0.25M sucrose, 0.5% 'Brij-35', pH 8.0 at 0°C) with six 30-sec passes of the pestle at 500 rpm. A supernate is obtained by slow-speed centrifugation, 10,000 g x 15 min

1003538671

Source: https://www.industrydocuments.ucsf.edu/docs/hgy10000

(International Equipment Co. #HT, #856 angle head), in the above buffer at 4°C. This is repeated, but at 35,000 *g*. The mitochondrial-free, nuclear-free, opalescent material obtained we term "ribo".

The above "ribo" is formed into a pellet in the above buffer (less 'Brij-35') and centrifuged at 105,000 g x 2 hrs at 4°C (International Equipment Co. #B-60, rotor #488). The pellet is gently resuspended in buffer and the procedure repeated. The final pellet is placed on a 5-20% sucrose gradient, non-linear in the 14-17% region as programmed from an ISCO Dialagrad #380 pump, and centrifuged in plastic tubes in the above rotor for 3 hrs at 45,000 rpm over a 2M sucrose cushion. The tubes are pierced from the bottom; the gradients are forced out by a flow of 2M sucrose from a Harvard pump, the flow is monitored by tandem ultraviolet recording sensors at 254 and 280 nm by an ISCO UA-2 #580 dual beam monitor, and about 30 fractions are cut by an ISCO #272 drop collector and carousel.

The methods given above are in fact a precis of those which we have successfully used and published previously. The fractions are then evaluated for their ribosomal content, ribosomal protein and ribonucleic acid, aspartic transcarbamylase, alkaline phosphatase, glutamyl transpeptidase and neurosecretory granules as outlined below.

b. Zonal ultracentrifugation:

The method for zonal preparation of particles is the technic of choice although, as explained above, its availability depends

1003538672

Source: http://www.industrydocuments.ucsf.edu/docs/[illegible]

upon mechanical function of an instrument which has worked well for others in the past but not us.

The preparation termed "ribo" (see a. 1. above) is used to load the zonal rotor (IEC #B-29), with the usual buffer system (see above). The sample is visibly marked through the introduction of blue Dextran, and injected at the core between a 5% sucrose layer beneath a 42 ml layer of 0-3% sucrose above.

The method of centrifugation is the new equivolumetric technic of Pollack and Price (54). In brief, it is required that there be a constant C such that:

$$C = \frac{r^2}{r \cdot n}(d_p - r \cdot d_m)$$

r = radial distance of particle from center
n = viscosity of sucrose buffer
d_p = density of particle (ribosome = 1.41)
d_m = density of sucrose buffer

They assume that a gradient can be designed such that a particle zone of zero radial thickness will migrate through equal volumes of gradient in equal increments of time. They do in fact demonstrate that for ribosomes loads of 5 mg or less, a particle zone of 10 ml or essentially negligible thickness may be obtained, which would for example give a resolution sufficient to separate 15-unit polysomes from 14-unit polysomes and 18S particles from 20S.

1. Enzymatic activity: the crude fractions, without further dialysis, concentration, nor clarification, which we term "cru-f", are tested for enzymatic activity with respect to alkaline phosphatase isoenzyme, g-glutamyl transpeptidase, and aspartic transcarbamylase. Since the methods used are exactly those outlined for serum enzymes under item (c. 2. Methods and materials) above, the technology will not be further discussed here.

10035386?3

Source: https://www.industrydocuments.ucsf.edu/docs/hqyl0000

2. Total protein: Aliquots of "cru-f" fractions are dialyzed exhaustively in a benzoylated membrane bag against distilled water and then tested for total protein by Lowry's method. When the results warrant, i.e. more than 20 ug protein, and if time permits, the protein is subjected to acrylamide gel electrophoresis in 7% gel at pH 8.4, for isoenzyme stains.

3. Neurosecretory granules:

(a) Wet chemical evaluation of bioamines from neurosecretory granules (51,56)

The technic is essentially that of Cottrell, i.e. sucrose gradient fractions are examined for bioamine activity by a fluorescence method (51). The fractionated homogenate (above) is extracted with 1:5 1N formic acid : acetone; the extract is dried in a stream of nitrogen and then briskly agitated in one volume of 0.01N HCl-saturated isobutanol for 5 min. Then, there is a second extraction with a 2X volume of low-fluorescence heptane during another 5-min. agitation period; the organic and aqueous phases then are separated at 1000 g x 5 min. The material of interest is placed on a 6 x 85 mm column of ion exchange resin (Amberlite CG-50, #2, 200-400 mesh) previously equilibrated with 0.2M phosphate buffer at pH 6.1, and is eluted with 1N HCl. General fluorometric conditions for analyses of the eluate are:

SUBSTRATE	PROCEDURE	FLUORESCENCE nm	
		ACTIVATION	EMISSION
5-hydroxytryptamine	5N HCl	300	545
Dopamine	Hydroxyindole (alkaline sulfate-acetic acid)	325	390
Noradenaline	Hydroxyindole (alkaline sulfate-acetic acid)	385	485

10035389274

Source: https://www.industrydocuments.ucsf.edu/docs/[illegible]

There are no innovations in this account from that published. In general, this method is considered to be a quantitative and specialized one, used as indicated to follow up upon the results of the screening test below. This method is precise at the nanomole range ± 10% approximately.

(b) Thin layer chromatography of bioamines from neurosecretory granules

An acid butanol extract, prepared as above, is spotted on thin layer plates of microcrystalline cellulose (Merck 'Avicel', without fluorescent indicator) and developed in the ascending mode with 60 : 20 : 20 isobutanol : methanol : 1N formic acid for four hours; the plates are dried at 56°C and redeveloped at right angles with 60 : 35 : 5 chloroform : methanol : 1N ammonium hydroxide for two hours.(47). The developed plate is reacted with paraformaldehyde vapors and fluoresced at 360 nm in order to locate the three major substrates. Alternately, all of the spots are developed with diazotized p-nitroaniline. This method is capable of resolving sixteen biologically significant amines, including many of the chief congeners of dopamine, 5-hydroxytryptamine, and noradrenaline, and including those three substrates themselve, and is sensitive in the nanomole range.

(c) Fluorescence of neurosecretory granules

The Falck-Hillarp method (45), of condensation with formaldehyde vapors to produce a fluorescent product in situ, is the method of choice and one we have observed in use (46). A recent minor modification of the method is selected (57). Cryostat microtome sections are prepared in 7% gelatin. Isopentane quenched material, at -170°C, is brought to -12°C, cut, and then dessicated at -60°C for three days at 0.001 torr with the aid of a Cenco pump and a Virtis dry-ice trap. It is then cut at 5 μ, and examined for fluorescence as in (5) a. 5. above.

10035386?5

Source: https://www.industrydocuments.ucsf.edu/docs/hhyd0000

4. Ribosome analyses:

These analyses depend upon the availability of the zonal ultracentrifugation head. In order for the ribosomes to be isolated by fractionation of the sucrose gradient as in item (5) c. above, and in accord with our published work (3, 50, 52), and marked with 'Blue' Sephadex, molecular weight 2,000,000.

The 83.5S peak, recognized from 254/280 nm dual channel records of the fractionated sucrose gradient (above) is formed into a pellet at 105,000 g x 5 hr in buffered sucrose in a swinging bucket head. The material is re-purified in this manner until the sample shows a 260/235 nm absorption ratio over 1.50, or it is rejected entirely.

The pellet is resuspended in a chelating buffer (0.02M $KHCO_3$, 0.001M HPO_4^- buffer at pH 7.3, 0.03M KCl, 0.004M ethylenediaminetetraacetate (EDTA)) to separate ribosomal subunits, and placed over a 10-20% sucrose non-linear gradient consisting of the above buffer plus 0.2M $MgCl_2$, less EDTA. This is spun at 110,000 g x 5 hr in an IEC zonal rotor #B-30. The 50S subunits (52), identified by the previously described ISCO dual channel recorder, are isolated by fractionation of the gradient, and dissociated in the above phosphate buffer plus 0.5M LiCl, 0.2M $MgCl_2$, and 6M urea.

This material is purified by zonal centrifugation at 150,000 g x 15 hr and dialyzed against 0.033M sodium acetate in 6M urea. The contents of the bag are concentrated when the bag is dehydrated in a bed of Sephadex G-200, and the product is electrophoresed on 12% acrylamide gel at pH 4.3 in the presence of 6M urea. The resultant bands are stained with Coomassie blue and read in our special integrating microphotomer (52).

1003538676

Source: https://www.industrydocuments.ucsf.edu/docs/nqyl0000

(3) Significance of work:

a. Defects in current experimental designs:

For years, we and many other anatomical pathologists have failed to develop models of lung injury which measure or correlate with actual physiological function. Equally, lung physiologists have avoided coming to grips with the alleged discrepancies between the histological appearance and micro-function of the injured lung. Indeed, micro-function --lobular function-- has hardly been studied by any discipline. And molecular biologists, excepting the few who deal with the specific problems of the type II cell, have conspicuously avoided molecular dissection and the cell biology of the lung.

Where does that leave us today? We stand on the verge of considerable advances in understanding how several important organs operate as systems: the brain, the kidney, the heart, several endocrine glands, and the liver -- but not the lung. In the list of tissues examined in dozens of monthly journals for this or that enzyme, organelle, or macromolecular product, or its regulatory actions, the lung is usually conspicucus by its absence. We want to remedy that situation. For several years, and mostly with the aid of The Council for Tobacco Research support, we have been attempting to develop a broadly based laboratory devoted to the systems analysis as well as the operational analysis of injured lung.

b. Systems analysis:

By systems analysis, we mean the study of the lung as an assemblage of modules and components, the interactions of which determine

1003538677

Source: https://www.industrydocuments.ucsf.edu/docs/mjyl0000

the function and fate of the injured organ. The key word is "interaction". In our model, we view the lung as a system of units, of which the incidental function is ventilation of the blood stream. Thus, the lung has the same needs for tissue homeostasis, for cellular nutrition, and for molecular regulatory mechanisms as the other organs in the body. To study the lung as organized around the air within it has no more rationale than to the study the heart as organized around the blood within it, or the kidney about the urine within it. To study the lung as a system, therefore, implies the capability and the confidence to relate its different tissue and cellular functions one to another -- or more briefly, to study the interactions. Thus, the multidisciplinary approach is intrinsic.

c. Operational analysis:

As to operational analysis, by this we mean a study of what the lung does. Again, we believe that the movement of blood and gases for ventilatory purposes is only one of many functions of the lung. But the first thing the lung does, to complement the above systems approach, is to keep itself alive and well as an organ. Therefore, from both the systems and the operational approach, we require that the lung be studied as tissue, with special recognition of its self-regulatory functions, its cellular biology, its macromolecular control mechanisms.

How do $\dot{V}/\dot{Q}$ defects relate to secretory molecular changes? How can defective tissue homeostasis result in a loss of bronchiolar compliance? Will bioamine-induced arteriolar tone modulate

100538678

Source: https://www.industrydocuments.ucsf.edu/docs/kbpf0068

the pumping of lymph? How does Clara cell function change with chronic obstructive airways disease? Is it inappropriate to speak of endexpiratory bronchiolar "collapse" when the role of the actively contractile bronchiolar muscle is not considered? What does the Kultschitsky cell do? Is there a calculus of lung function, i.e. does the lung function as a mass organ or as an integrated collection of subunits? What is the effect of destroying the integration function, if it exists, as opposed to destroying discrete anatomical targets? Are there valid computer models for self-regulating lung functions? The answers to these questions are perforce interdisciplinary, and cannot be studied outside of a systems framework, in an operational manner.

d. Immediate significance:

Thus, a major immediate significance of our work lies in its innovative approach to the lung. It would not be revolutionary in the study of, say, transport of salt by frog bladder, or, for example, memory by brain tissue. But applied to lung, the approach is most uncommon.

In an operational and systems context of a real laboratory, the revolution turns out to be unexpectedly simple in concept. It asks that we study sick animals in much the same way that we study sick humans. We would not presume to follow a patient seriously ill with bronchitis without complete blood counts, clinical chemistry and blood gas studies, periodic measurements of pulmonary function, and chest roentgenographs.

10035386?9

Source: https://www.industrydocuments.ucsf.edu/docs/boyl0000

We propose to follow sick animals the same way. To this we add the possibilities of a more thorough autopsy study because with animals, unlike with humans, we can secure necropsied tissue with almost no autolytic artefacts. So the "new" approach is as conservative as it is revolutionary. It is nothing more than the application of the principles of sound clinical judgment to the evaluation of a sick patient. It is in itself an exploration of what is clinically relevant in experimental airways obstruction, an attempt to get input for human disease on a rapid basis.

e. Long range significance:

The ultimate significance has the possibility to be quite large.

First, if the approach is successful, it would change the style of some other researchers from monodisciplinary to multidisciplinary.

Second, it would systematically apply a tremendous amount of clinical knowledge and equipment -- multiphasic screening comes to mind -- to the management of experiments in which the animals are supposed to be models of sick humans; thus, a larger yield of directly useful clinical insights might come to light.

Third, and possibly most important, it would provide a means to understand the lung as a lung, and not as a collection of type II cells, or regional areas of poor air exchange, or thrombosed arteries, or whatever the glaucomatous monodisciplinary approach focuses upon.

10035386680

Source: https://www.industrydocuments.ucsf.edu/docs/hcyl0089

Fourth, we would understand the lung as a system of total pathology. Our one team of investigators, working with one animal model, will build up within its own members various centers of specialization: physiological, histopathological, and biochemical. These functions complement and mirror the similar tripartite functions of a clinical pathologist in his daily work-- and it is a clinical pathologist who who is senior investigator. So another significant product is the entry of clinical pathology into the fundamental research on lung disease. By professional necessity, this specialist is accustomed to thinking of the patient in broad terms, inclusive of formal histopathology but also of the biochemistry of body fluids and the physiological function of organs and systems.

Indeed, the molecular fractionation of homogenized lung, and the serial examination of such fractions for their relevant enzymatic, macromolecular, and neurohumoral components is very much along the line of multiphasic screening. The major difference is, we have chosen to measure moities that we suspect in advance of having important cellular roles for lung function, growth, injury, and repair.

Ordinarily, to achieve these magnitudes of significance would be impossible on the proposed operational funding basis within the specified time. In this case, NIHL has generously funded a team which is laying the groundwork for every area outlined in the proposal above except those in which The Council for Tobacco Research, through previous support, has already provided us with facilities and expertise. The only new endeavor is with reference to neurosecretory granules.

1003538681

Source: https://www.industrydocuments.ucsf.edu/docs/hqyl0000

f. Summary:

The overall significance, we hope, will be to turn lung researchers and clinicians away from monodisciplinary studies towards multi-disciplinary ones; away from consideration of the lung as a breathing bag and towards consideration of it as a tissue with all the homeostatic, regulatory, and macromolecular functions an organ requires to maintain its own autonomous existence; away from passive models of lung function towards those in which muscle contraction, tissue metabolism, and neurohumoral secretion are intrinsic to functional activity; away from emphasis on the alveolar transfer function of the lung and towards emphasis of bronchiolar function, compliance, and gas-mixing properties; away from a philosophy of mass lung action and towards one in which unit lobules dominate lung activity in the same way that unit nephrons dominate renal activity.

10035386B2

(4)

PROJECTED SCHEDULE OF LABORATORY WORK

PHASE	MONTH	DUTIES FOR PERSONNEL
START-UP	1	Advertise positions; interview and hire candidates. Order equipment. Begin technical training. Breed guinea pigs.
TRIALS & DEVELOPMENT	2-3	Dry runs on molecular biology. Practice runs on autopsy/histology. Develop neurosecretory granule fluorescence technic.
	4-8	Practice runs on total experiment.
	9	Feedback modulation of experimental design.
EXPERIMENTS	10-14	First series of experiments: cycle 1 oxygen toxicity, 20 guinea pigs, fixed starting age.
	15	Finish enzyme work on frozen extracts of gradient fractions.
	16	Calculation of results. Write paper. Feedback modulation of experimental design.
	17-23	Repeat cycle 1
	24-30	Second series of experiments: cycle 2 oxygen toxicity, 20 guinea pigs, various starting ages (effects of growth on injury and repair)
	30-36	Third series of experiments: cycle 3 Tobacco induced alterations, 20 guinea pigs (correct model to be chosen from cycle 1 or 2 above) Final report.

	FULL-TIME DUTIES OF PERSONNEL
Biologist:	Does tests for and evaluates clinical data. Breeds animals, keeps records, assists in autopsies and histopathology. Does mucus cell counts and tantalum macrophage counts, assists physiologist, prepares fluorescence specimens for pathologist. Serves as group leader.
Physiologist:	Runs blood gas station, does multichannel physiological testing, maintains equipment, evaluates data, performs computations, assists biologist and/or chemist.
Chemist:	Performs gradient fractionations, enzymatic analyses, ribosomal analyses, thin layer chromatograms, evaluates data.

10035386B3

Source: https://www.industrydocuments.ucsf.edu/docs/[illegible]

(5) INTERPRETATION OF RESULTS

This will be considered under 4 subheadings: molecular, morphological, clinical, and theoretical. In reality, the experiments are performed as a whole, and there are not separate experiments in each category. Animal models will be examined at 4 days, 2 weeks, and 4 months, which are respectively interpreted as acute, subacute, and chronic.

a. Molecular:

1. Ribosomal activity and protein synthesis:

It is assumed that the three proteins considered, the enzymes glutamyl transpeptidase, alkaline phosphatase, and aspartyl transcarbamylase, are produced by ribosomes in the classic manner.

(a) Glutamyl transpeptidase: studies on liver (58) or isoenzymes (59) suggest strongly that this cytoplasmic enzyme appears in the serum during the early phases of cellular damage. Thus, we shall try to correlate quantitatively levels of this enzyme in homogenized fractionated lung with levels of it in the serum during injury and repair. In addition, we hope to pinpoint the locus of intracellular synthesis pari passu, since the fractionating procedure deals simultaneously with enzymes, subcellular particles (such as vesicles derived from rough endoplasmic reticulum), polysomes, and ribosomes. This remarkable capability is inherent in the process of zonal ultracentrifugation. Hence, the interpretation of results deals with molecular events in the cell in terms of their morphological consequences, and holds possible advances both in clinical and theoretical knowledge.

10035538684

Source: https://www.industrydocuments.ucsf.edu/docs/hpn79000

(b) Aspartyl transcarbamylase: this enzyme is nucleus-related, for it is an obligate part of the DNA synthesis chain. Whereas DNA may also be studied directly (by thymidine labeling) with the indirect aspartic transcarbamylase technic it may prove possible to infer, from serum changes, events which occur in an organ. Thus, enzyme levels in serum will therefore also be correlated with their corresponding tissue values and their location during fractionation procedures, as above.

(c) Alkaline phosphatase: just as glutamyl transpeptidase is a marker for injury, and aspartic transcarbamylase for cellular regeneration, alkaline phosphatase is a marker well known for its association with differentiated mucosal cell activity. Results of all three enzymes will be interpreted in this light. In addition, because the alkaline phosphatase enzyme system is so well known, there are ready methods for its histochemical and serum isoenzymatic analyses, both of which we propose to do. Thus, the differentiation of cells containing alkaline phosphatase will be studied from the histochemical and as well the subcellular aspects, and also with respect to isoenzyme where that seems feasible. Since the differentiated function of the bronchiole includes, we believe, airways regulation, these data will also be correlated with lung function studies.

(d) Ribosomal protein: We have conclusively showed the regular appearance of abnormal constitutive ribosomal protein early in lung injury with oxygen. We shall continue to use it as

10035388685

Source: https://www.industrydocuments.ucsf.edu/docs/[illegible]

a marker in this way. It will be of great interest to correlate changes in enzymatic spectrum with changes in ribosomal structure. If we are lucky, we may get some clues to the molecular nature of the abnormally dense contents of rough endoplasmic reticulum (of Clara cells) which appear during the first week of oxygen intoxication (7,20) and probably other lung injury.

2. Neurosecretory granules: whereas proteins and ribosomes are intricately related, the subcellular site of Kultschitsky cell active secretion is extra-ribosomal and is unknown. Our first interpretations, then, will be addressed towards the subcellular localization of these granules in molecular dissections on the ultracentrifuge and correlated by light and electron microscopy; and second, we shall interpret regenerative and synthetic activity of the various hydroxyindole family members with the state of lung injury and repair. These interpretations will be colored by our notion that the neurosecretions may play a regulatory role in the maintenance of lung lobular homeostasis and/or function, themselves measured by lung function as well as molecular enzyme studies.

b. Morphological

1. Fluorescence microscopy: this is the qualitative tissue method for citing the localization and distribution of neurosecretory granules isolated on the ultracentrifuge.

2. Electron microscopy: this is a consultative service, the function of which is to provide the morphological correlation for the molecular processes measured above. Pictures will be interpreted qualitatively, with special regard to mucosal cell patterns, and to distribution of neurosecretory granules.

100353868

Source: https://www.industrydocuments.ucsf.edu/docs/hgyl0000

3. Light microscopy:

(a) Tantalum in macrophages: this is interpreted as a means of roughly gauging lung clearance, and based on quantitative counts.

(b) Goblet cell counts: these are interpreted as indicative of the animal equivalent of human mucus gland counts. Chronically increased numbers of goblet cells are interpreted as indicative of chronic bronchitis.

(c) Semiquantitative graded lesions: these form the basis for considering whether our animals have in fact developed comparable lesions. We assume, in the interpretation, that there are some true parameters and some independent variables. This ordinal grading is a parameter. Only animals with similar toxic dose histories and similar grading will be compared. (Past experience has been that correlation coefficients of the order of 0.9 are possible if graded bronchiolar morphology is compared to oxygen dose.)

c. Physiological ("clinical") lung tests:

1. Nitrogen washout procedures: These are interpreted with respect to regional disorders, the numerical lesions above, and molecular bronchiolar changes. The oxygen washout measured by the high-speed analyzer is the inverse of the nitrogen washout, as discussed above, and nitrogen washout is a time-honored method for the determination of regional $\dot{V}/\dot{Q}$ anomalies. This is a particularly reasonable approach in the guinea pig lung, because the collateral air circulation (pores of Kohn) is poorly developed in these animals (60). Thus, the guinea pig should emphasizes, by nature's design, factors that lead to lobular airways obstruction.

100538687

Source: https://www.industrydocuments.ucsf.edu/docs/[illegible]

2. Minute ventilation: integration of the total tidal exchange per minute, as measured by a body plethysmograph, provides this datum. Incidental to this, the breathing frequency is also provided. These data are cross-correlated with nitrogen washout primarily, and with molecular and histocytological data secondarily.

d. Chest roentgenographs: Insofar as feasible, these are interpreted as the in vivo counterparts to histological examination and particularly subgross anatomy, at the bronchiolar level, and correlated with these.

e. Complete autopsy procedures provide a measure of comparability of the accumulated clinical data obtained during one life, and both sets of information are useful in establishing the comparability of measurements in serried experiments. This is quite important, because the experimental design calls for the continuance sequencing of pairs of guinea pigs rather than mass experiments on a large number of guinea pigs at once.

1003538688

Source: https://www.industrydocuments.ucsf.edu/docs/[illegible]

(6) PREVIOUS WORK

Previous advances made possible in our laboratory by dunded support, exclusively by The Council for Tobacco Research, have been molecular, morphological, and theoretical. However, before the current proposal, we had no means of physiologically testing any practical conclusions made as a result of our studies.

a. Molecular:

We have demonstrated that, contrary to expectations based on early histochemical work (Sorokin), there is a sharp drop in ribosomal synthesis in lungs of normal newborn guinea pigs a few days after birth (50). These observations themselves devolved from the creation of a whole technology in the molecular dissection of lungs, one in which our laboratory seems to be foremost at present (3 ,50,52, 53,61,62,63). With this technic, we were able to demonstrate that ribosomal synthesis is turned on by mucosa soon after the destructive lesions of pulmonary oxygen intoxication. Moreover, we showed that ribosomes of injured lungs differ molecularly from normal ones through electrophoretic differences in the constitutive basic protein of the ribosome, a finding of fundamental importance throughout the field of cell biology. Experiments to localize the findings to ribosomal subunits have not as yet been decisive. Lately, we have correlated distribution of the isoenzymes of alkaline phosphatase with these ribosomes in growing and injured lung (4). Results thus far show rather pronounced shifts in the subcellular distribution of alkaline phosphatase, absolutely as well as relatively, some of which seem related to ribosomes. Three different species of rodent -- rabbit, rat, guinea pig -- share some similarities. Most intriguing is the

1003538689

Source: https://www.industrydocuments.ucsf.edu/docs/kqyl0000

observation that the mass of an individual class subcellular alkaline phosphatase particle generally increases with age, and also that some particle sizes seem to have characteristic locations in terms of Svedberg ultracentrifugation. Figs. 15-20.

b. Morphological:

The bronchiolar injuries of oxygen have been clearly documented in rat (20), mouse (49), guinea pig (7), and human (21). This is a unique contribution of our group, since all other investigators of oxygen intoxication have concentrated upon alveoli instead of bronchioles. Our studies have included ultrastructure also (20,64). We have showed the progression of the oxygen-induced lesions, and in particular, have documented the important role played by bronchiolar reaction and metaplasia in airways obstruction (20), a role for which exfoliative cytology provides a handy clinical foil (65). We developed the first concept of oxygen "dose". Under the impetus of these studies, we proposed a semiquantitative ordinal grading system (Fig. 14) for evaluation of lung morphology which helps eliminate observer bias in the comparison of histological lung findings. This system is a direct outgrowth of a similar one used in the evaluation of bronchopulmonary dysplasia (oxygen intoxication of the newborn), the study which led to our Council for Tobacco Research support (21). In addition, we have completed the first survey by any group of the developmental and ultrastructural morphology of human bronchioles (11). Currently, we are summarizing a portion of this work in each of three different review volumes (13,14,15). Figs. 21-26

c. Clinical:

The clinical dangers of oxygen for the lungs of newborns were first explained by us (66). Subsequently, we coined the term "bronchopulmonary dysplasia" as

1003538690

Source: https://www.industrydocuments.ucsf.edu/docs/hqyl0000

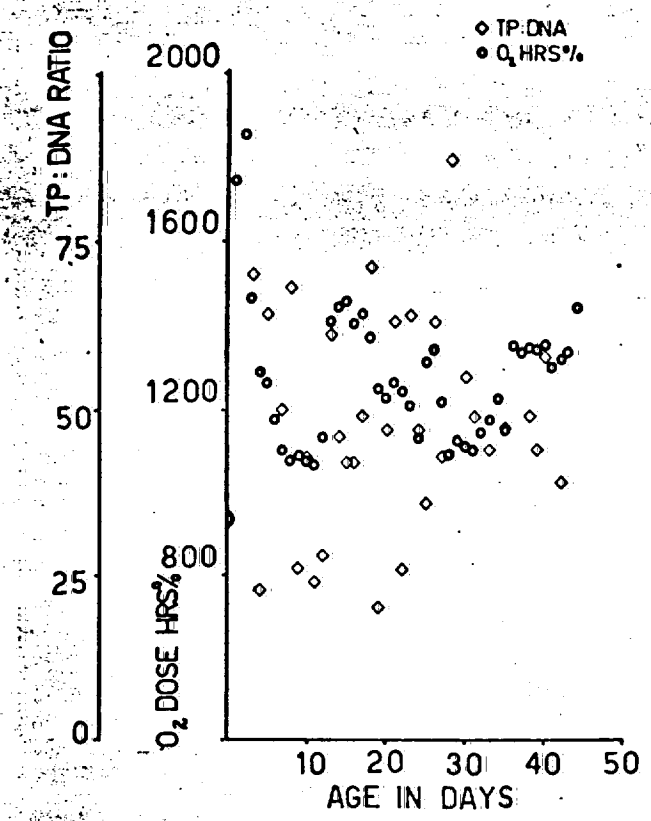

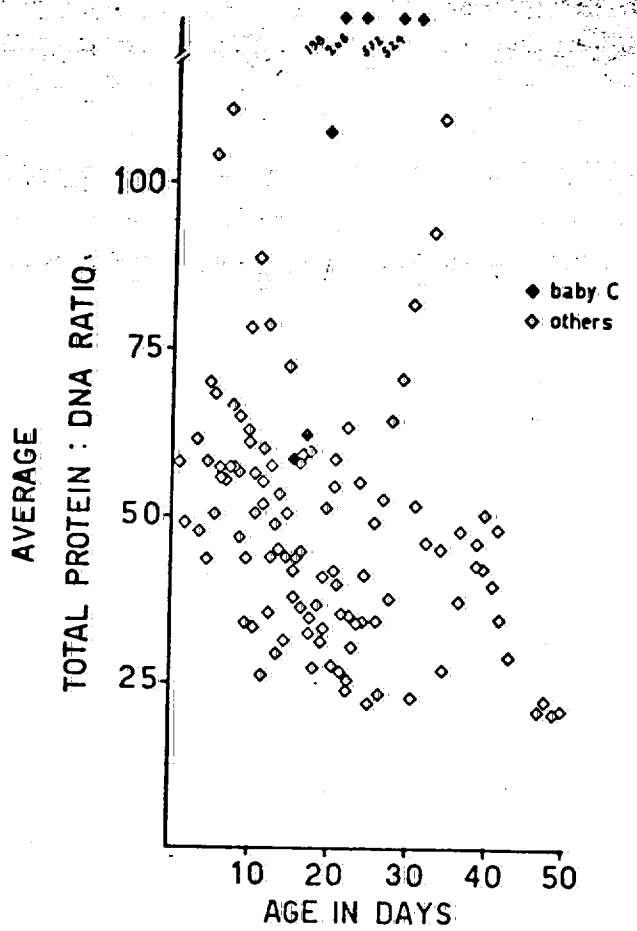

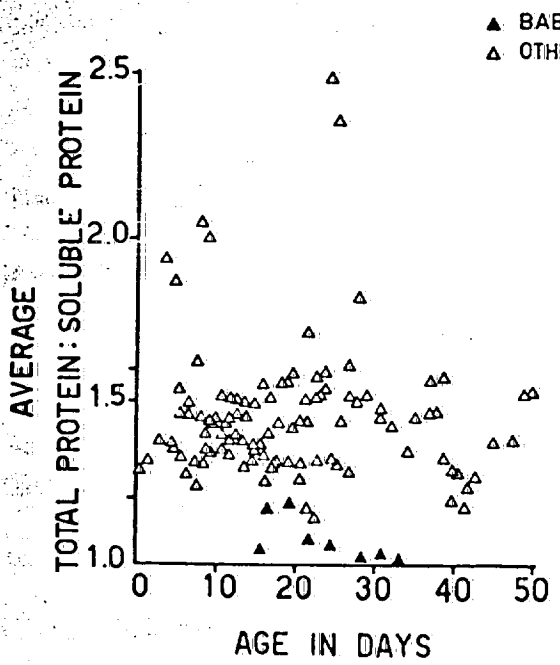

Fig. 21 COMPARISON OF BIOCHEMICAL VARIATIONS IN 24 HR POOLS OF ENDOTRACHEAL SECRETIONS IN 5 BABIES WHO DIED AND ONE WHO SURVIVED AFTER OXYGEN THERAPY.

Upper left: Baby C has least oxygen dose

Upper right: Baby C secretes much more protein than DNA. This tends to show that oxygen necrotizes cells.

Lower right: Baby C secretes much more soluble than insoluble protein; the latter is associated with increased production of mucus and fibrin.

Conclusion: There may be an association between the biochemical and clinical effects of oxygen toxicity.

Added note: Cytological analyses of the above secretions showed many mucosal cells with atypia present (as well as lining cells from other lung regions.)

1003538691

Source: https://www.industrydocuments.ucsf.edu/docs/hqyl0000

FIGS. 22, 23, and 24: With collaboration of J M Lauweryns.

OXYGEN INTOXICATION OF THE END-BRONCHIOLE OF THE NEONATAL GUINEA PIG (Composite photograph)

This picture develops within 4 days of the start of 100% oxygen therapy at controlled humidity. We believe that the extensive damage to the "valve" area of the bronchiole is much like that seen in humans. In Fig. 22, which is a montage of several photographs, the swollen smooth muscle on the extreme sides of the picture is of note, as well as the necrotic mucosal, Clara, and ciliated cells. In Figs. 23 and 24, the damaged Clara cell is seen, and the characteristic rough endoplasmic reticulum with its dense fibrillogranular contents is apparent. Mitochondria are known to be easily injured by oxygen; and the close association of (?regenerative?) ribosomal organelles with injured mitochondria is often seen in these experiments.

Fig. 22

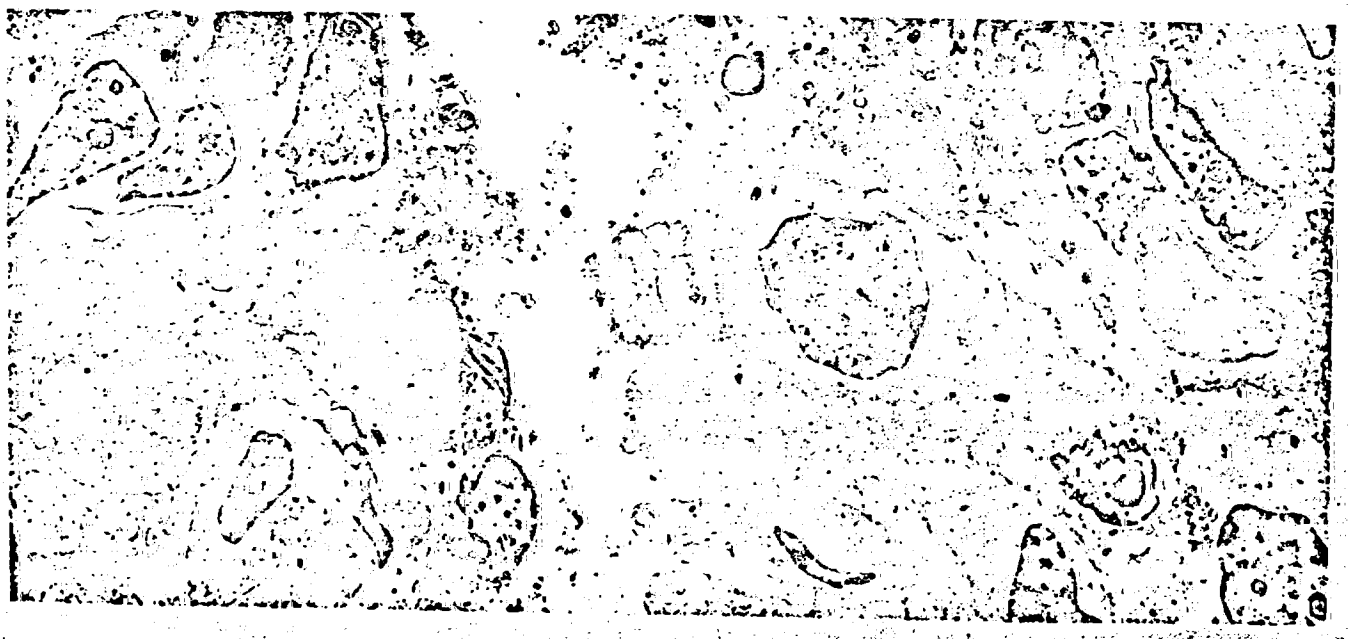

10035386 92

Source: https://www.industrydocuments.ucsf.edu/docs/xyc0000

Fig. 23

Fig. 24

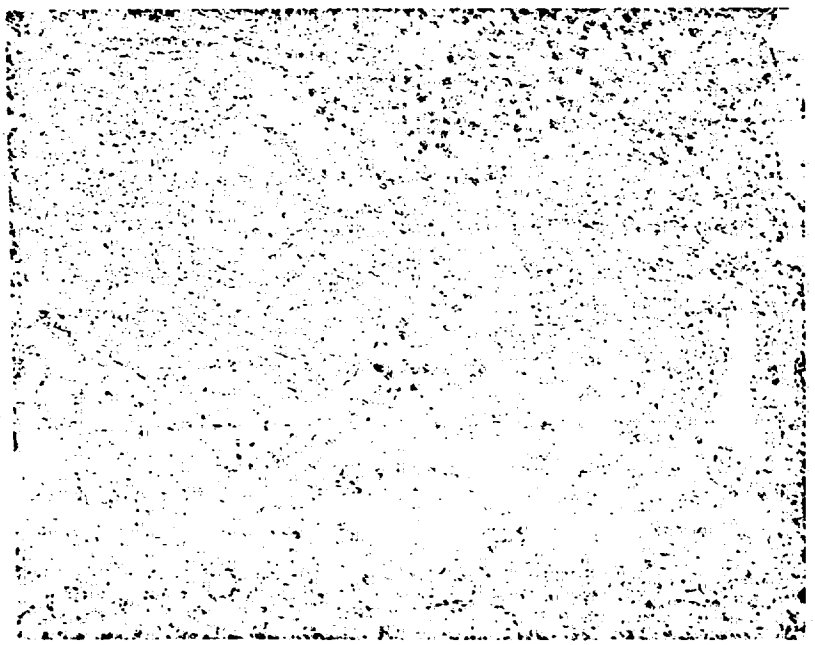

10035386 93

Source: https://www.industrydocuments.ucsf.edu/docs/hgyl0000

descriptive of this rather characteristic condition (21) and the term is slowly coming into usage. We have documented that airways obstruction may begin in newborns and leave chronic residual disease (67). We have showed how roentgenological details may be followed with regard to prognosis (68), and the same for exfoliative cytology (65). The molecular pathology of the secretions has been explained (28). Even in our first full report, we had developed an ordinal grading method for interlaboratory comparison (21). Along the way, we have tested and rejected the notion that hyaline membrane disease is a sequel to morphological brain injury, and developed the first systematic neuropathology for long-term survivors of that condition (29). More recently, we worked out the difference in morphology between long survivors who do and who do not have a history consistent with oxygen intoxication. It turns out that hyaline membrane disease alone may heal by a type of chronic interstitial pneumonitis, whereas bronchopulmonary dysplasia is associated with chronic obstructive airways disease, chronic pulmonary hypertension, and chronic metaplastic lesions of the bronchioles (21,69). In view of the importance of juvenile chronic bronchitis to adult obstructive lung disease, we think these are significant observations. Figs. 21,25,26,28

d. Theoretical:

One major contribution has been the idea of the unit lobule (10,14), a rather unique solution to many of the problems which arise in the interpretation of neonatal lung disease and its sequelae. Briefly, this theory lays heavy stress on the importance of the bronchiolar components of the ontogenetic lobule for regulation of air, lymph, and blood flow (10,11,15), and also the intersaccular septa (which are the unique infantile lung structures described by Professor J. M. Lauweryns) for the modulation of mechanical and homeostatic behavior.

100353869

Source: https://www.industrydocuments.ucsf.edu/docs/hgyl0000

The theory emphasizes consideration of the lung as tissue. The emphasis on bronchiolar compliance has recently been supported by in vivo measurements of infants in our clinic, which have shown compliance of so great a magnitude that carbon dioxide retention and ventilatory ("dead-space") acidosis are regular concomitants of some types of positive end-expiratory ventilation. The last is itself a clinically significant observation. It is interesting that our theory feelings converge with those recently expressed by J. M. West: ".....a cynic might say that only a respiratory physiologist with his obsession for simple diagrams could picture an alveolus as a balloon on a tube exposed to pleural pressure." (60). That "tube" and the regulation of its compliance will be, we believe, among the principal areas of advance in the next few years of lung research. We specifically postulate that injuries to lung during the neonatal period of rapid growth may lead, in some cases, to life-long pulmonary handicaps and a predisposition to chronic airways disease. Figs. 27, 28.

10035388695

Source: https://www.industrydocuments.ucsf.edu/docs/[illegible]

Fig. 25

Saccular portion of the normal lobule of the prematurely born infant (c. 600 g)

Especially noteworthy are the thick "intersaccular septa", the well-developed and almost mature air-blood barrier portion of the capillary-epithelial junction, the numerous glycogenolated "cuboidal" cells, and the neurosecretory cell which is far from any observable mucosa (circle).

By collaboration with J M Lauweryns

100353696

Source: https://www.industrydocuments.ucsf.edu/docs/hqjl0000

Fig. 26

Destruction of the saccular portion of the neonatal lobule after more than 250 hr of 100% oxygen with assisted ventilation.

By collaboration with Gladys Harrison.

Especially noteworthy is the disappearance of air-blood barriers, cellular atypia, and prominent interstitial collagenization.

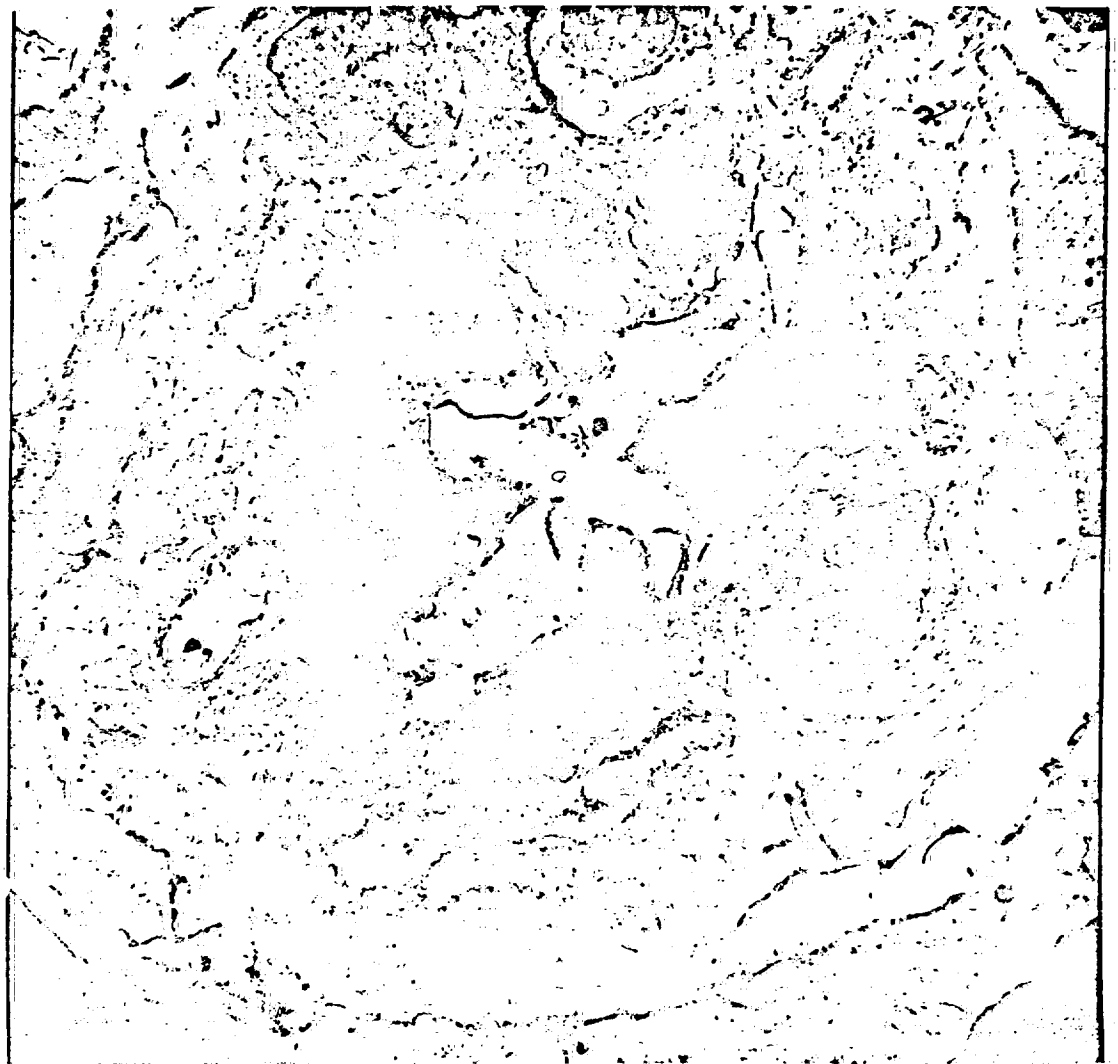

1003538697

Source: https://www.industrydocuments.ucsf.edu/docs/hqyl0000

FIG. 27

Breath-by-breath analysis (retracing of actual record) of oxygen extraction from normal room air for an adult guinea pig. The scimitar-shaped tracings are an artefact of the (non-rectilinear) Harvard Apparatus Company's pen-amplifiers, and would be replaced in the current proposal.

The record shows the practicality of making fast oxygen measurements in the plethysmograph (see Fig. 8) used in this project. The shape of the decay curve, after 5 minutes of breathing 100% oxygen, can be measured easily as these data--which were secured after breathing room air--show.

If the oxygen extraction by a guinea pig lung can be measured at his nose, it should be practical to do the same for patients. Thus, it might be possible to envision a non-invasive continuous monitoring system for patients taking physiological function tests, or for those who must receive mechanical ventilation.

1003538698

Source: https://www.industrydocuments.ucsf.edu/docs/hdjl0000

1003538699

Source: https://www.industrydocuments.ucsf.edu/docs/hqyl0000

FIG. 28

Effect of positive end-expiratory pressure on bronchiolar compliance

This figure shows the importance of an appropriate lung model to clinical medicine. The results below should not occur in a surfactant theory.

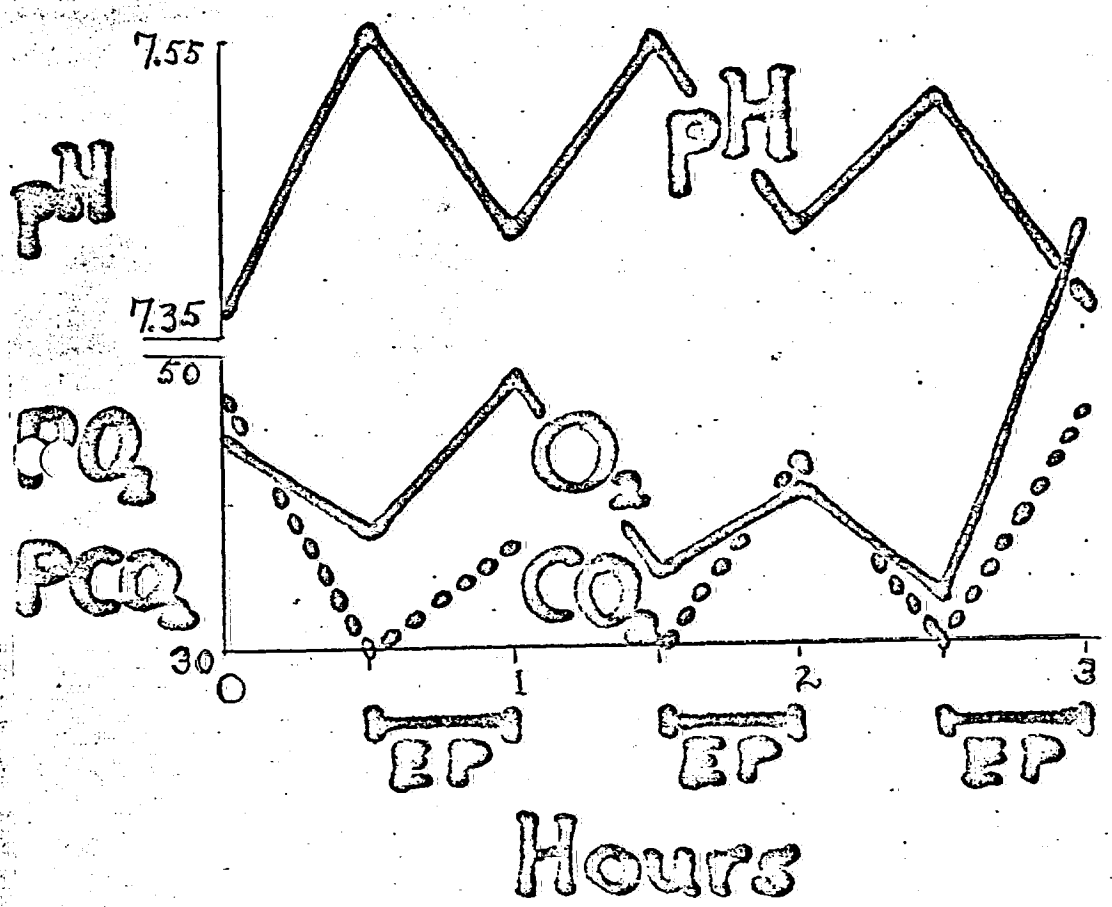

The application of end-expiratory pressure continuously for half hour periods (about 6 mm H_2O pressure) helps drive oxygen into the lung, for the P_aO_2 increases. However, the pressure also increases P_aCO_2 by virtue of increasing the bronchiolar "dead-space". The net effect may actually worsen the acidosis as above. However, this latter is unusual. What the experience demonstrates is that the neonatal bronchiole is highly compliant. In this the case, the patient weighed about 1200 g.

1003538200

Source: https://www.industrydocuments.ucsf.edu/docs/hqyf0000

FIG. 29

Flow Diagram for Isolation of Ribosomal Proteins from Subunits Derived from Newborn Human Lungs

Liq. N_2-frozen lung, extruded in Arbor Press

5ml D-"B"/ g lung tissue

Homogenize, 500 rpm, 6- 30 second strokes

8k-G x 12 min.

Sediment

Supernate

25k-G x 12 min.

Sediment

Supernate

Cheesecloth

Over 2ml D-"B" in 2M sucrose

105k-G x 5 hrs.

Pellet

Supernate

Resuspend in D-"B" and D-"E", 1:1

Over 2ml D-"B" in 2M sucrose

Pellet

Supernate

Resuspend in 0.5ml of:
0.02M $KHCO_3$
4.0mM EDTA
1.0mM Phosphate Buffer, pH 7.3
0.03M KCl

Over Sucrose Gradient:
10-20% sucrose
1.0mM Phosphate Buffer, pH 7.3
0.03M KCl
0.2mM $MgCl_2$

110k-G x 5 hrs.

Fractionate @ 280nm, Flow-cell, ISCO UV Analyzer

Subunits, 50S and 30S

Preparation of Monosomes

Preparation and Separation of Ribosomal Subunits

1003538701

Source: https://www.industrydocuments.ucsf.edu/docs/hqyl0000

Flow Diagram, continued

50S Subunits

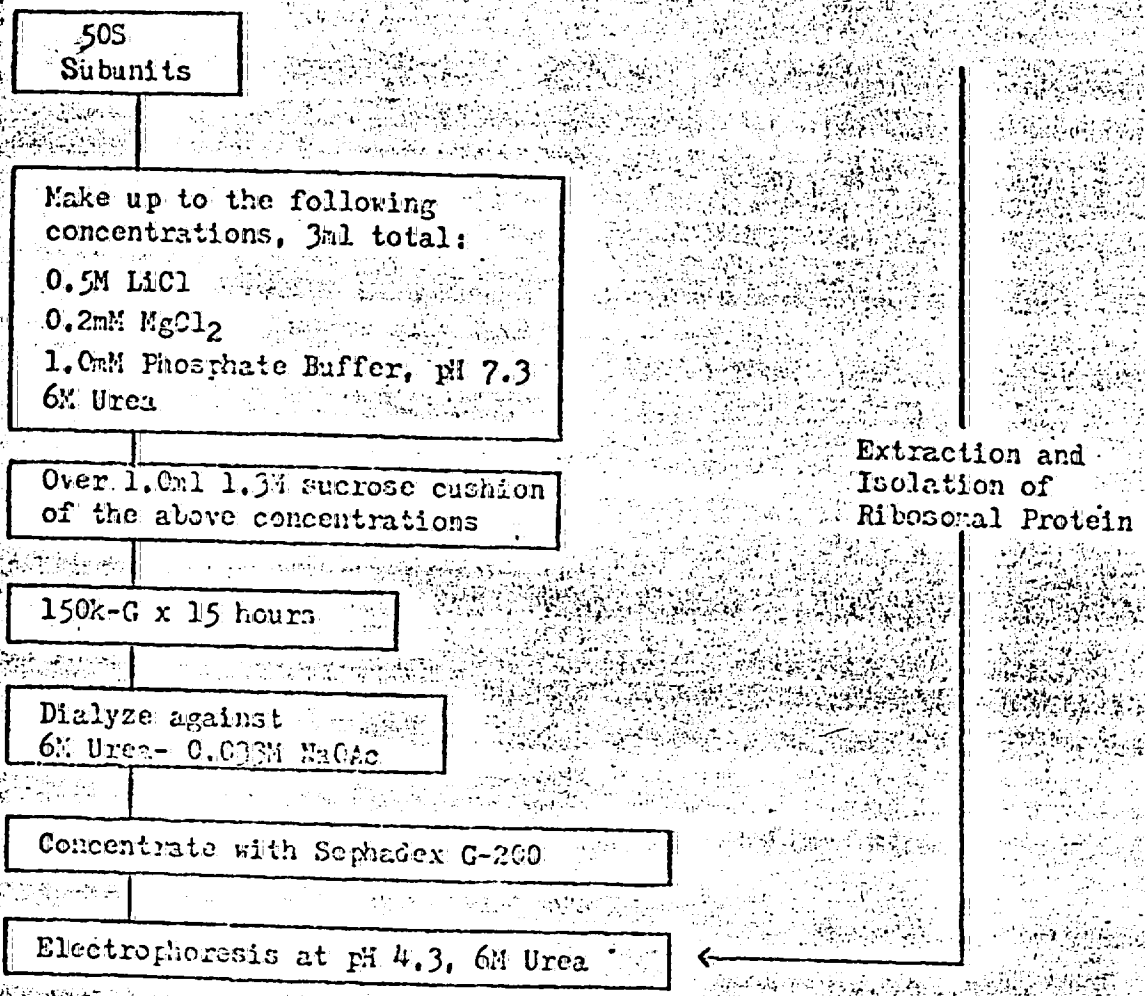

Make up to the following concentrations, 3ml total:
0.5M LiCl
0.2mM $MgCl_2$
1.0mM Phosphate Buffer, pH 7.3
6M Urea

Over 1.0ml 1.3M sucrose cushion of the above concentrations

150k-G x 15 hours

Dialyze against 6M Urea- 0.033M NaOAc

Concentrate with Sephadex G-200

Electrophoresis at pH 4.3, 6M Urea

Extraction and Isolation of Ribosomal Protein

References

M. M. Bieber, M. G. Cogan, T. C. Durbridge, and R. C. Rosan
Biol. Neonat. 17: 35-43, 1971

Rebound, Hamilton, and Petermann
Biochem. 8: 843-850, 1969

1003538702

Source: https://www.industrydocuments.ucsf.edu/docs/mgjb0000

REFERENCES

1. Histochemical and biochemical investigations of Gamma-glutamyl transpeptidase in the tissues of man and laboratory rodents
Albert, Zygmunt, Orlowska, Jadwiga, Orlowski, Marian, and Szewczuk, Apolinary
Acta Histochem. 18: 78-89, 1964

2. Aspartate transcarbamylase
Porter, R. W., Modebe, M. O., Stark, G. R.
J. Biol. Chem. 244: 1846-1859, 1969

3. Changes in ribosomes from neonatal animal lung following 98% oxygen exposure *
Durbridge, T. C., Cogan, M. G., Bieber, M. M., and Rosan, R. C.
Naturewissen 58: 456-457, 1971

4. Macromolecular dissections of newborn human and animal lung
Suen, J-S, and Rosan, R. C.
Fed. Proc. 31: 642, 1972

5. Single breath analysis of oxygen exchange in guinea pig pups
Nixon, J. M., Champagne, G. J., and Rosan, R. C.
In progress

6. Powdered Tantalum as a medium for bronchography in canine and human lungs
Nadel, J. A., Wolfe, W. G., and Graf, P. D.
Invest. Radiol. 3: 229-233, 1968

7. Radiologic and histologic investigation of pulmonary oxygen toxicity in newborn guinea pig
Northway, W. H., Jr., Rosan, R. C., Shahinian, L., Jr., Castellino, R. A., Gyepes, M. T., and Durbridge, T. C.
Invest. Radiol. 4: 148-155, 1969

8. Experimental bronchitis in animals due to sulphur dioxide and cigarette smoke. An automated quantitative study.
in "Inhaled Particles. III." Ed by Walton, W. H.: pp 509-525
Unwin-Gresham. Surrey. 1971

9. The fine structural localization of biogenic monoamines in nervous tissue
Bloom, F. E.
Internat. Rev. Neurobiol. 13: 27-66, 1970, Ed. by Pfeiffer, C. C. and Smythies, Jr.

10. The unit lobule: a revised concept of the neonatal lung
in "Perinatal Medicine" Ed by Huntingford, P. J., Beard, R. W., Hytten, F. E., and Scopes, J. W.: pp 259-261, Proc. 2nd Europe Congr. Perinatal Med.
S. Karger, Switzerland, 1971

11. Mucosal cells of the small bronchioles of prematurely born human infants (600-1700 g) *
Rosan, R. C., and Lauweryns, J. M.
Beitr. Arch. 147: 145-174, 1972

10035387203

Source: https://www.industrydocuments.ucsf.edu/docs/hgyl0000

12. "Hyaline membrane disease" in newborn infants
Lauweryns, J. M.
Human Pathol. 1: 176-204, 1970

13. Recent advances in pathological aspects of neonatal respiratory distress *
Rosan, R. C., and Lauweryns, J. M.
Pathol. Ann. 8: 1976 (accepted)

14. Bronchopulmonary dysplasia and infantile chronic lung disease
in "Review of Pediatric Pathology" Ed by Rosenberg, H., and Bolande, R.

15. Neonatal bronchioles
Rosan, R. C.
in "Anatomy of The Lung" Ed by Wilson, J.

16. Surface phenomena in health and disease
Avery, M. E., and Said, S.
Med. 44: 503-512, 1965

17. Auerbach, O.
Personal communication, 1972

18. Thurlbeck, W.
Personal communication, 1972

19. Strang, L.
Personal communication, 1970

20. Experimental bronchiolitis induced by acute and chronic oxygen intoxication of young adult rats *
Harrison, C., Rosan, R. C., and Sloane, A.
J. Path. 102: 115-121, 1970

21. A new syndrome of pulmonary disease following respirator therapy of hyaline membrane disease : bronchopulmonary dysplasia
Northway, W. H., Jr., Rosan, R. C., and Porter, D. Y.
N. Engl. J. Med. 276: 357-368, 1967

22. "Fysiologie en Pathologie in de Perinatale Periode" pp 34-35
in Pathologisch Anatomische Bevindegen Bij Kunstmatic Beademde pasgenborn in Boerhave Curssussen voor Voortgezet Medisch Onderwijus
Gaillard, J. L. J.
Rijksuniversiteit, Leiden. Nederlands, 1969

23. The fetal and neonatal lung
in "Biology of Gestation", vol. 2. Academic., N.Y., Ed by Assali, N. S. 1968
Towers, B.

1003538704

Source: https://www.industrydocuments.ucsf.edu/docs/hgg0000

24. Acidosis and positive end-expiratory pressure
Byrne, P., and Rosan, R. C.
In progress

25. Zur Histobiologie des bronchialepitheliels
Clara, M.
Ztschr. f. mikr - anat. Forsch. 41: 321-347, 1937

26. L'angioarchitecture du poumon
Lauweryns, J. M.
Arch. Biol. (Suppl.) 75: 771-787, 1964

27. Towers, B.
Personal communication, 1972

28. Oxygen pollution; its effect on the ecology of lung cells
Rosan, R. C., and Lauweryns, J. M.
Naandschr. Kindergenees. 39: 143-161, 1971

29. Neuropathological lesions in respiratory distress syndrome: Acute and chronic changes during hypoxia and oxygen therapy
Brand, M. M., Durbridge, T. C., Rosan, R. C., and Northway, W. H., Jr.
J. Reprod. Med. 8: 267-279, 1972

30. The biochemical development of surface activity in mammalian lung. II. The biosynthesis of phospholipids in the lung of the developing rabbit fetus and the newborn
Gluck, L., Sribney, M., and Kulovich, M. V.
Ped. Research 1: 247-265, 1967

31. Macromolecular dissections of newborn human and animal lung
Suen, J-S, and Rosan, R. C.
Fed. Proc. 31: 642, 1972

32. Distribution of alkaline phosphatase in lungs
Pounds, G. W., Lee, J-S., and Rosan, R. C.
In progress

33. Histochemical and biochemical investigations of Gamma-glutamyl transpeptidase in renal cancer of man
Albert, Zygmunt, Orlowska, Jadwiga, and Orlowski, Marian
Acta Histochem. 18: 90-94, 1964

34. A kinetic photometric method for serum γ-Glutamyl transpeptidase
Szasz, Gabor
Clin. Chem. 15: No. 2, 124-136, 1969

35. Lactic acid analysis by 2-wavelength enzymatic technic on ABA-100
McEwan, S. N., Gagen, H., and Rosan, R. C.
Abstr. Centr. Ind. Clin. Biochem. For., Indianapolis, 1972

10035387O5

Source: https://www.industrydocuments.ucsf.edu/docs/[illegible]

36. Aspartate transcarbamylase
Collins, Kim, D., and Stark, George, R.
J. Biolog. Chem. 244: 1869-1877, 1969

37. "The Lung"
Comroe, J. H., Jr., Forster, R. E., II, Dubois, A. B., Briscoe, W. A., Carlsen, E.
2nd Ed. pp 65-69. Yearbook, Chicago, 1970

38. Analytical cytology of mucin production. Mucinous cytoplasmic granules in a myxomatous tumor of hamster
Rosan, R. C., and Spring, E. J.
J. Histochem. Cytochem. 11: 414-419, 1963

39. Mechanism of the differential staining reaction for adrenaline and noradrenaline storing granules in tissues fixed in glutaraldehyde
Coupland, R. E., and Hopwood, D.
J. Anat. 100: 227-243, 1966

40. The use of lead citrate at high pH as an electron-opague stain in electron microscopy
Reynolds, E. S.
J. Cell Biol. 17: 208-213, 1963

41. On improved phase microscopy of tissue cultures
Rosan, R. C.
J. Histochem. Cytochem. 11: 557-559, 1963

42. Sigma Tech. Bull. #85

43. A direct lead method for the electron microscopic visualization of alkaline phosphatase activity
Hugon, J., and Borgers, M.
J. Histochem. Cytochem. 14: 429-431, 1966

44. Cytochemical and ultrastructural observations on the argentaffin and argyrophil cells of the gastrointestinal tract in mammals and their place in the APUD series of polypeptide-secreting cells
Carvalheira, A. F., Welsch, U., and Pearse, A. G. E.
Histochem. 14: 33-46, 1968

45. The formaldehyde fluorescence method for the histochemical demonstration of biogenic amines: a review of methodology
Corrodi, H., and Jonsson, G.
J. Histochem. Cytochem. 15: 65-78, 1967

46. Argyrophil (kinin and amine producing ?) cells in human infant airway epithelium
Lauweryns, J. M., and Peuskens, J. C.
Life Sci. 8: 577-585, 1969

10035387206

Source: https://www.industrydocuments.ucsf.edu/docs/hgyl0000

47. Quantitative thin-layer chromatographic estimation of labeled dopamine and norepinephrine, their precursors and metabolites
Fleming, R. M., and Clark, W.
J. Chromatog. 52: 305-312, 1970

48. Experimental bronchiolitis induced by acute and chronic oxygen intoxication of young adult rats *
Harrison, G., Rosan, R. C., and Sloane, A.
J. Path. 102: 115-121, 1970

49. Chronic oxygen toxicity in newborn mice
Northway, W. H., Jr., and Rosan, R. C.
to be published

50. Oxygen toxicity in the newborn guinea pig: the incorporation of tritiated uridine into monoribosomes *
Bieber, M. M., Cogan, M. G., Durbridge, T. C., and Rosan, R. C.
Biol. Neonat. 17: 35-43, 1971

51. Isolation of dense-cored granules from the neurosecretory system of the vena cava of the small octopod, Eledone cirrosa
Berry, Cynthia, F., and Cottrell, G. A.
Br. J. Pharm. 40: 549-551, 1970

52. Small-scale molecular dissections of ribosomes of newborn guinea pig lung (NGPL)
Heldt, G. P., and Rosan, R. C.
Fed. Proc. 30: 194, 1971

53. Effect of oxygen on ribosome labeling of newborn guinea pig lung
Bieber, M. M., Rosan, R. C., Durbridge, T., and Harrison, G.
Fed. Proc. 28: 686, 1969

54. Equivolumetric gradients for zonal rotors: separation of ribosomes
Pollack, Marilyn, S., and Price, C. A.
Anal. Biochem. 42: 38-47, 1971

55. Pharmacological significance of biogenic amines in the lungs: noradrenaline and dopamine
Aviado, Domingo, M., and Sadavongvivad, Chiravat
Br. J. Pharmac. 38: 374-385, 1970

56. Individual elution of noradrenaline (together with adrenaline), dopamine, 5-hydroxytryptamine and histamine from a single, strong cation exchange column, by means of mineral acid-organic solvent mixtures
Atack, C. V., and Magnusson, T.
J. Pharm. Pharmac. 22: 625-627, 1970

57. Localization of monoamine-containing neurones in the nervous system of strophocellus oblongus (Gastropoda)
Jaeger, C. P., Jaeger, E. C., and Welsh, J. H.
Z. Zellforsch. 112: 54-63, 1971

10035387

Source: https://www.industrydocuments.ucsf.edu/docs/hqyl0000

58. Comparison of the diagnostic value of serum alkaline phosphatase and y-Glutamyl transpeptidase in biliary obstruction
Lukasik, Seweryn, and Richterich, Roland
Archivum Immunolo. Ther. Experi. 13: 580-585, 1965

59. Heterogeneity of human y-Glutamyl transpeptidase studied by Sephadex gel filtration
Orlowski, Marian, Szczeklik, Andrzej, and Kolaczkowska, Barbara
Archivum Immunolo. Ther. Experi. 13: 564-572, 1965

60. Respiration
West, J. B.
Ann. Rev. Physiol. 34: 91-116, 1972

61. Isolation of ribosomes from guinea pig (GP) lungs
McQuillan, J. E., Cogan, M. G., and Rosan, R. C.
Fed. Proc. 27: 541, 1968

62. Effect of oxygen on ribosome labeling of newborn guinea pig lung
Bieber, M. M., Rosan, R. C., Durbridge, T., and Harrison, G.
Fed. Proc. 28: 686, 1969

63. Oxygen-induced bronchiolar changes in infancy
Rosan, R. C., Durbridge, T. C., and Bieber, M. M.
Arch. Dis. Child, 45: 710, 1970

64. Oxygen-induced lesions in newborn guinea pig bronchioles
Rosan, R. C., and Lauweryns, J. M.
submitted for publication

65. Oxygen therapy hazards in the neonate
Northway, W. H., Jr., and Rosan, R. C.
Hospital Pract. 4: 59-67, 1969

66. Pulmonary dysplasia following survival from severe respiratory distress syndrome (RDS) of newborn: a new disease?
Rosan, R. C., Porter, D. Y., and Northway, W. H., Jr.
Fed. Proc. 25: 603, 1966

67. Rapid growth and centrolobular emphysema after stenosing tracheitis and continuous exposure to low concentrations of oxygen
Bieber, C. P., Rosan, R. C., Northway, W. H., Jr., Smith, P. C., Daily, W. J., and Brand, M. M.
Acta Paed. Scandinav. 59: 697-700, 1970

68. Radiological features of pulmonary oxygen toxicity in the newborn: bronchopulmonary dysplasia
Northway, W. H., Jr., and Rosan, R. C.
Radiology 91: 49-58, 1968

69. Chronic bronchitis and hyaline membrane disease
Saier, F. L., and Rosan, R. C.
Abstr. Ped. Pathol. Soc., Washington, D.C., 1973

1003538708

Source: https://www.industrydocuments.ucsf.edu/docs/hqyd0000